Rock Mechanics and Radioactive Waste Isolation.
"One small step for geology, one giant leap for rock mechanics"

Fourth Müller Lecture

presented by

Charles Fairhurst

Professor Emeritus, University of Minnesota, U.S.A.
Senior Consultant, Itasca Consulting Group, Inc.
Minneapolis, MN 55401, U.S.A.
fairh001@umn.edu

Tenth Congress of the International Society for Rock Mechanics
Sandton, South Africa, September 8-12, 2003

International Society for Rock Mechanics

Early Members

1 - Prof. Leopold Müller, Austria
2 - Mr. F. Pacher, Austria
3 - Prof. L. V. Rabcewicz, Austria
4 - Mr. C. Lorber, Austria
5 - Prof. F. Kahler, Austria
6 - Dr. W. Zanoskar, Austria
7 - Mr. W. Finger, Austria
8 - Dr. A. Fuchs, Austria
9 - Prof. F. K. Müller, Austria
10 - Mr. P. Reska, Austria
11 - Dr. K. Waschek, Austria
12 - Prof. G.B. Fettweis, Austria
13 - Dr. Georg Beurle, Austria
14 - Neue, Reformbaugesellschaft MbH, Austria (Supporting Member)
15 - Dr. Alois Kieser, Austria
16 - Prof. H. Seelmeier, Austria
17 - Dr. Adolf Bretterklieber, Austria
18 - Mr. W. Wessiak, Austria
19 - Prof. A. Watznauer, East Germany
20 - Prof. Charles Fairhurst, USA

Journal

FELSMECHANIK UND INGENIEURGEOLOGIE

ROCK MECHANICS AND ENGINEERING GEOLOGY

CONTINUING GEOLOGIE UND BAUWESEN FOUNDED BY J. STINI

JOURNAL OF THE INTERNATIONAL SOCIETY OF ROCK MECHANICS

HERAUSGEGEBEN VON / EDITED BY
L. MÜLLER
SALZBURG

UNTER MITWIRKUNG VON / IN COOPERATION WITH
C. FAIRHURST
MINNEAPOLIS

VOL I/1
(GEOLOGIE UND BAUWESEN Jg. 28/2)

SPRINGER-VERLAG WIEN 1963

Ph.D. degrees in Rock Mechanics, University of Minnesota (1960-2003) & Departmental Colleagues & Associates

1960-1969:

Paul Gnirk
Bezalel Haimson
William Hustrulid
Hassan Imam
Herbert Kutter
William Pariseau
Hilmar von Schoenfeldt
Wolfgang Wawersik

1970-1979:

Francois Cornet
Steve Crouch
Jaak Daemen
Michael Hardy
John Hudson
Darrell Porter
Jean-Claude Roegiers
Raymond Sterling
Ed Van Eeckhout
Michael Voegele

1980-1989:

Gary Callahan
Christine Detournay
Emmanuel Detournay
Roger Hart
Jose Lemos
Ernest Lindner
Loren Lorig
Panos Papanastasiou
Samuel Sharp
Yongjia Wang

1990-present:

Jose Adachi
Margaret Asgian
Nathali Boukpeti
Ilya Berchenko
Bjorn Birgisson
Mark Board
Roberto Carbonell
Carlos Carranza-Torres
Fernanda Carvalho
Liangsheng Cheng
Branko Damjanac
Ali Fakimi
Dimitri Garagash
Matt Handley
Haiying Huang
Mark Larson
Chengho Lee
Marc Loken
Mark Mack
Sanchai Maitaim
Lee Petersen
Thomas Richard
Robert Santurbano
Alexei Savitski
Sakir Selcuk
Eduard Siebrits
Ketan Shah
Keh-Jian (Albert) Shou
You Tian
Yiming Sun
Jeff Whyatt

Honorary Members:

Randall Barnes
Barry Brady
Ted Brown
Neville Cook
Peter Cundall
Andrew Drescher
Bojan Guzina
Joe Labuz
Tom Lang
Yoshi Mizuta
Chuck Nelson
Anthony Pearson
Fritz Rummel
Miklos Salamon
Chris St. John
Tony Starfield
Otto Strack

ITASCA

MTS Professorship

The problem. Waste Decay

- Contains the byproducts of fission reactions.
- Is highly radioactive.
- Must be isolated from the public for many thousands of years.

Needed 1 million year radionuclide ‘container’

Geological Isolation?

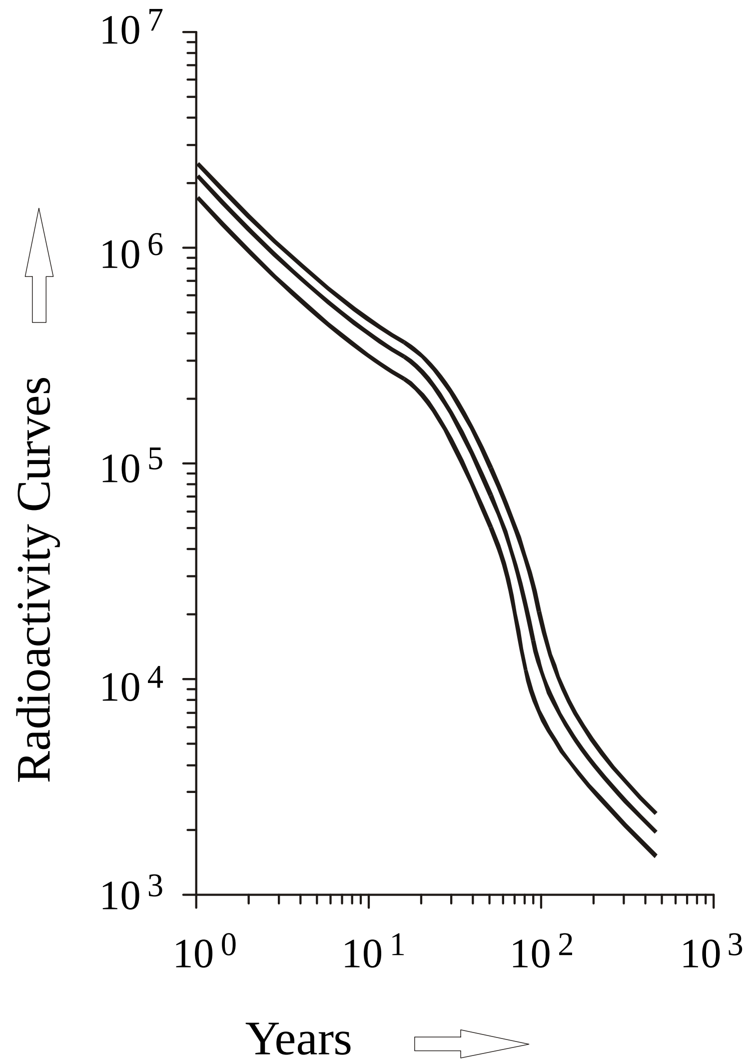

Alternative hypothetical extrapolations of
cancer death rate curves from high to
low radiation dose rates

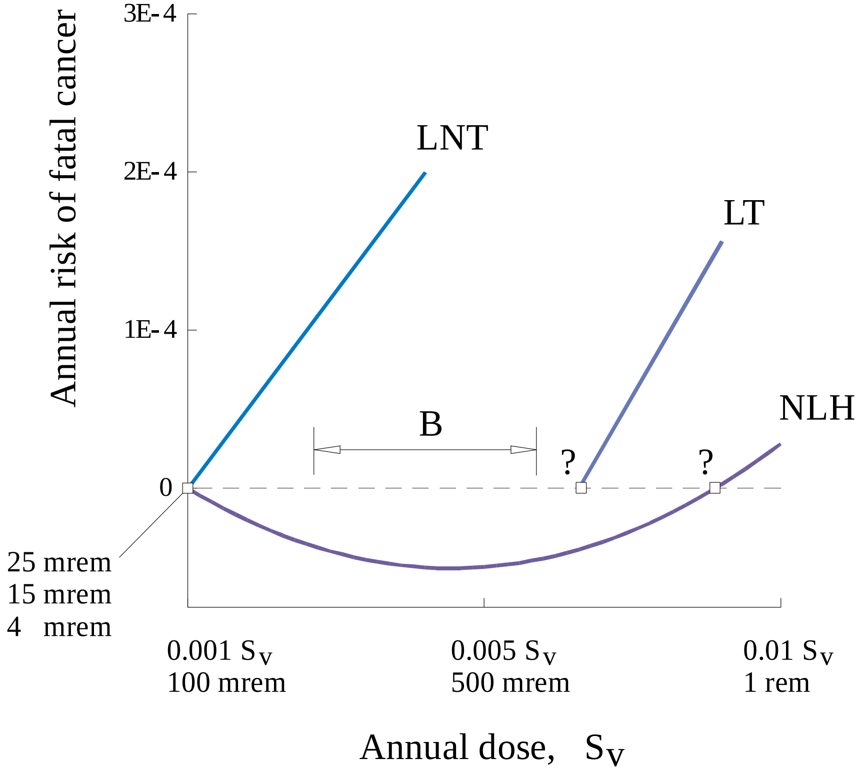

Dose-response relationships for solid cancer,
all types combined, in atomic bomb survivors,
1958-1987 (from UNSCEAR, 1994)

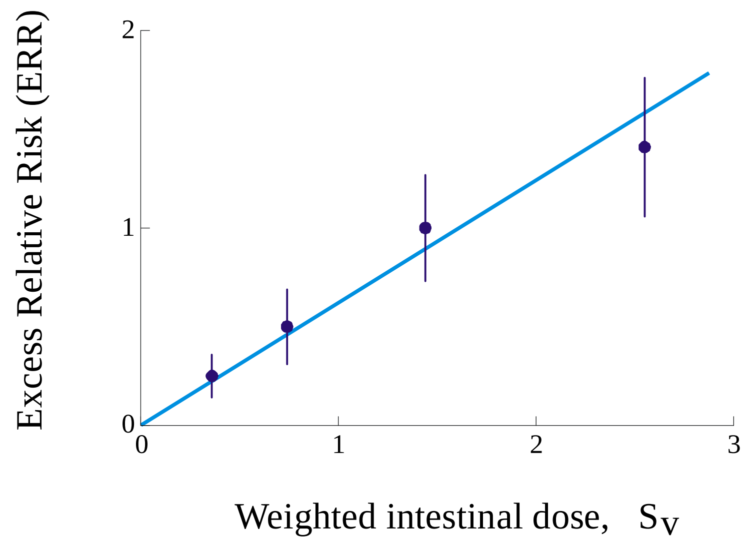

LNT Linear, no threshold
LT Linear, threshold
NLH Non-linear, Hormesis
B Range of natural background radiation in U.S. (approximate)

Radiation Risk and Waste Isolation Standard. LNTH and Natural Background

Risk of death from radiation

Global Dose rates from Natural Background Radiation

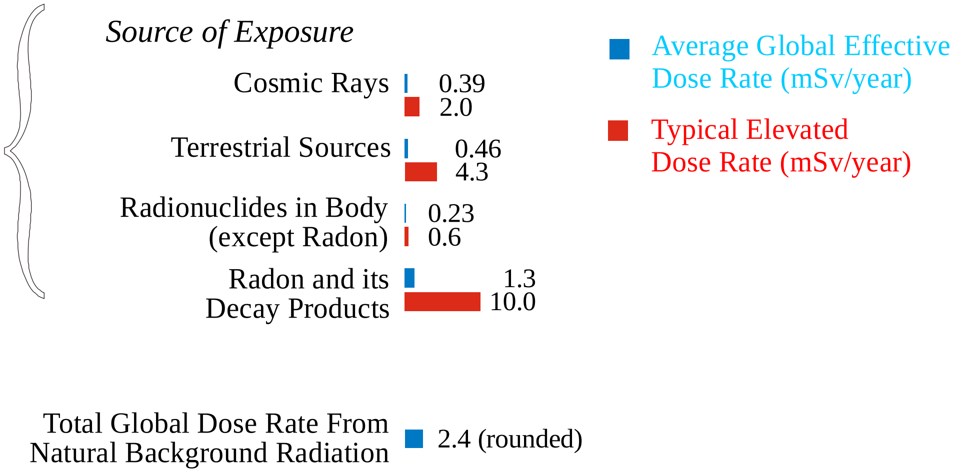

Reference:
ICRP, 1999. "Protection of the Public in Situations of Prolonged Radiation Exposure," Publication 82, Annals of the ICRP, Vol. 29, Nos. 1-2, International Commission on Radiological Protection, Pergamon Press, New York, NY. Table A.1, page 73, and Table A.2, page 74.

Examples of Areas with High Natural Background Dose Rates

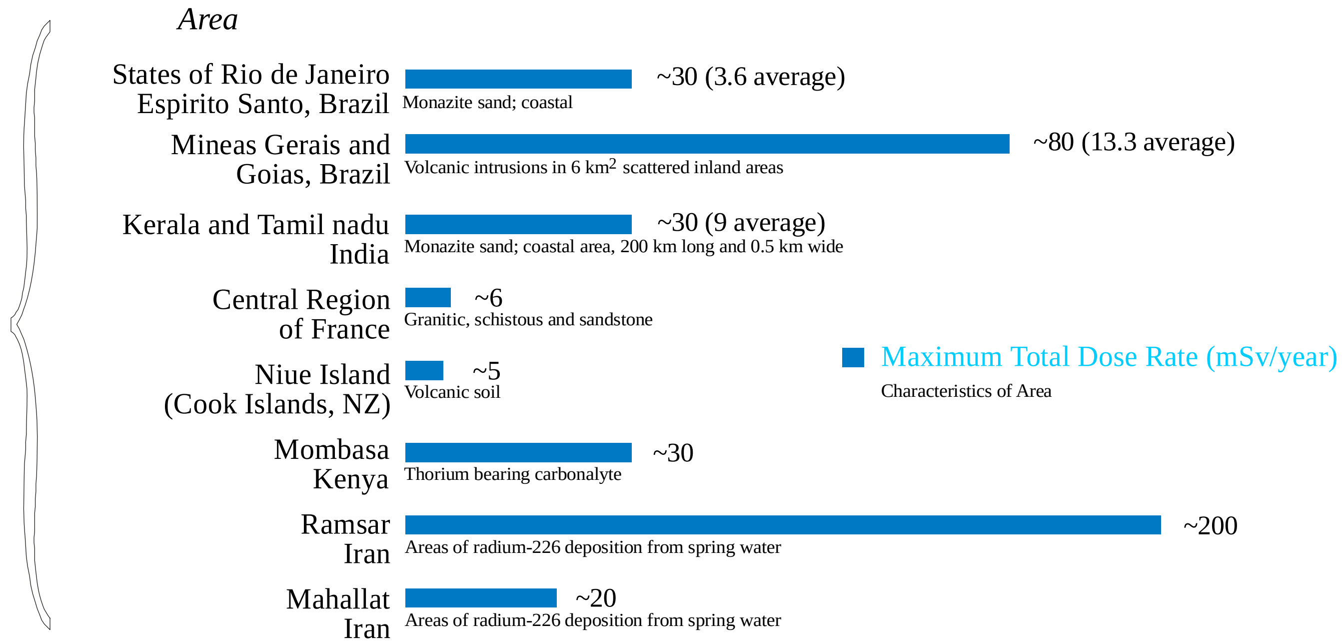

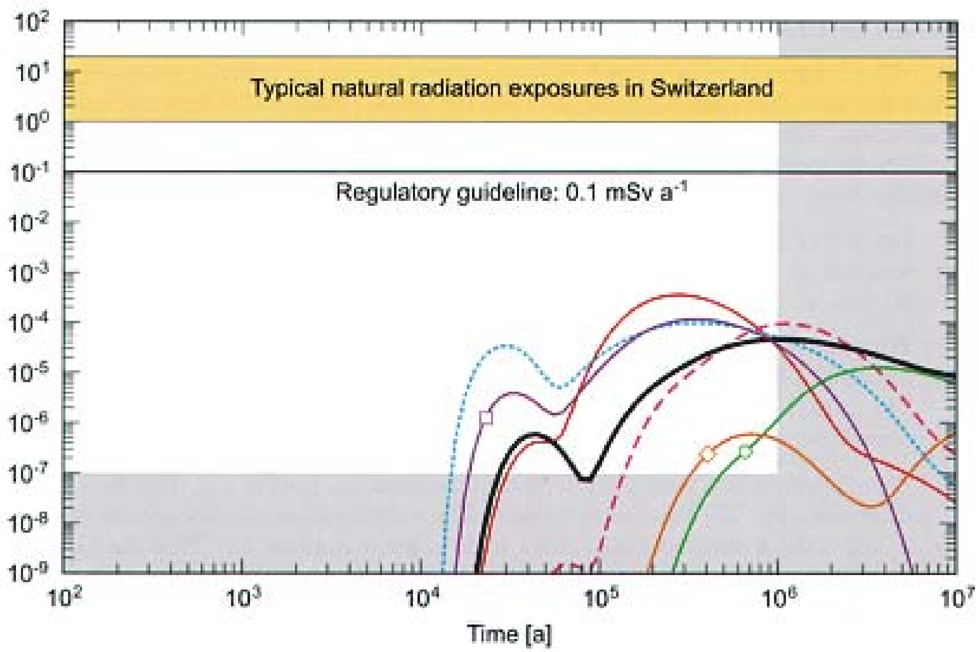

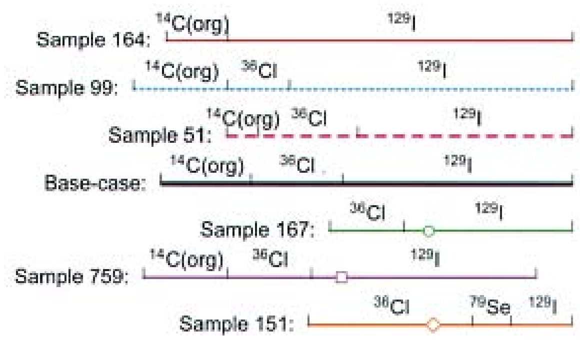

Dose as a function of tume, for SF, for a number of different realisations, including those that gave the highest (sample 164) and the lowest (sample 151) dose maximum out of 1000 realisations.

The Base Case is included to allow an easy comparison. The other curves represent realisations that give the highest dose maximum or the lowest dose maximum in the period between 10^4 and 10^5 years or 10^6 and 10^7 years, respectively. The bars beneath the graph indicate the radionuclides that make the highest contribution to dose at any particular time.

Predicted Performance of a Repository in Opalinus Clay Spent Fuel
—from *NAGRA Technical Report* 02-05, p.229

“One small step for geology, one giant leap for rock mechanics”

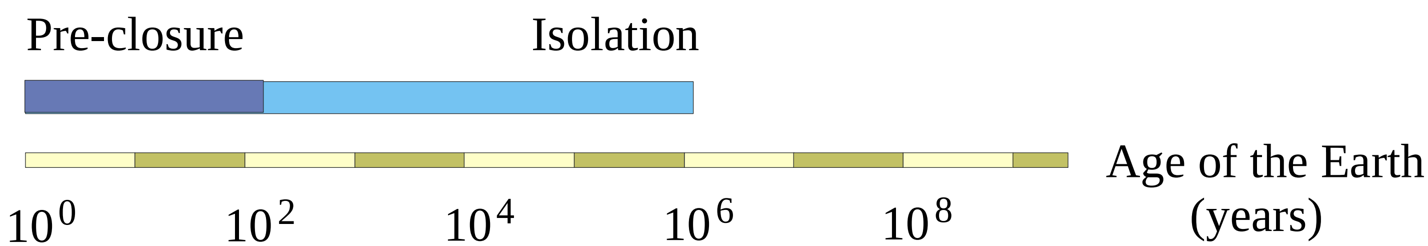

- Engineering Problem

  Unprecedented Period of Time

  Requires Improved Scientific Base

Periods of Isolation. Geological Isolation Time Scales.

“We don’t know the rock mass strength. That is why we need an International Society” Muller, 24 May 1962

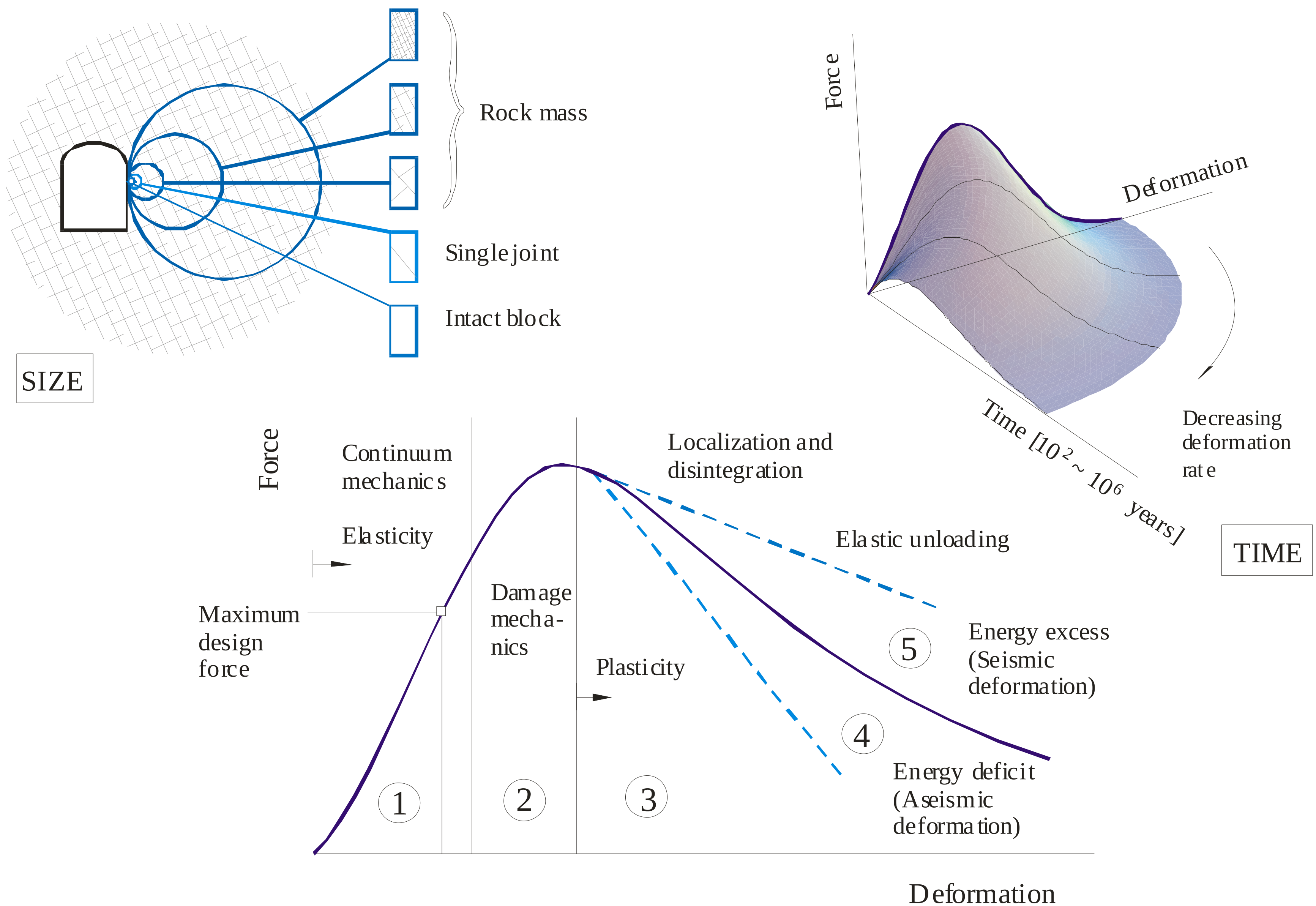

Complete Load-Deformation Behavior

"In the field of geomechanics, granular media and block-jointed rock masses are obvious examples where the concept of the ideal physical continuum – one in which no gaps are formed – cannot be expected to apply... The clastic model offers an alternative approach.

Indeed, it is this writer's view that only with clastic models or some further development thereof can the problem of predicting the complete load-deformation behaviour of solids be tackled optimistically."

D.H. Trollope (1968)

Geological Isolation

Choose a geologically simple, stable site!
(low tectonic strain rate)

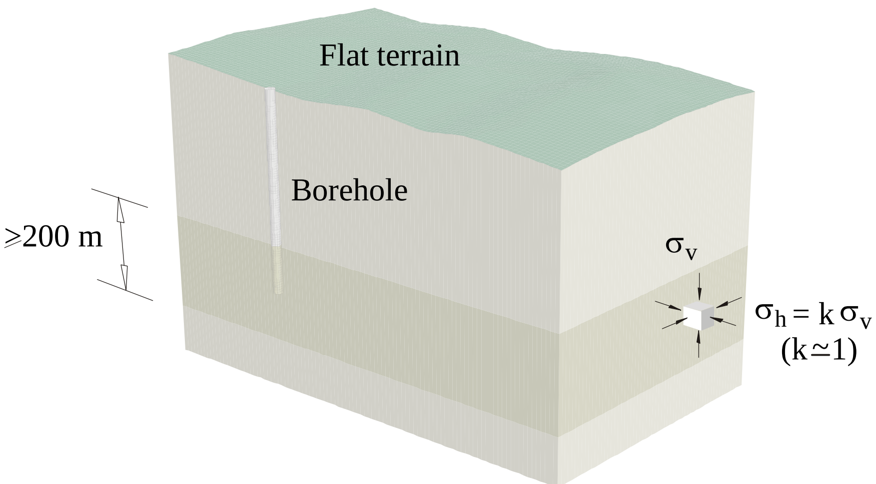

Overlying and underlying strata:

- Infrequent joints/faults.
- Far-field stresses close to isotropic.
- Groundwater discharge to large body of non-potable water (ocean, sea).

Repository stratum, simple host medium::

- Low permeability.
- Low hydraulic gradient.
- High ion-exchange potential.

Establish and close the repository

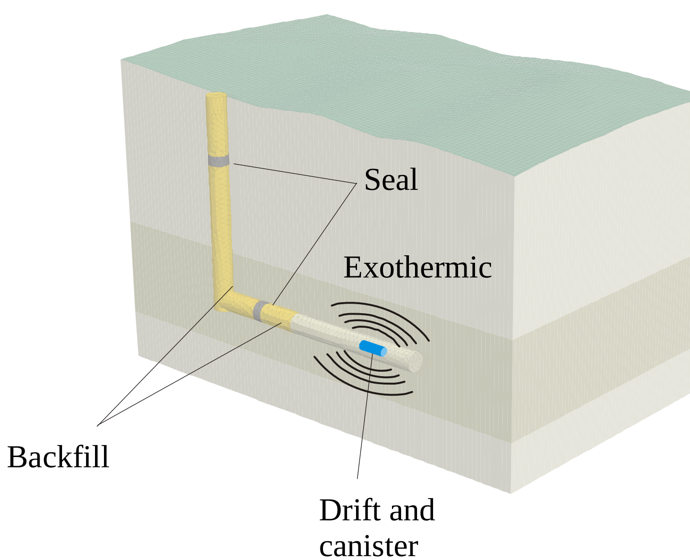

Detail of
seal and
backfill

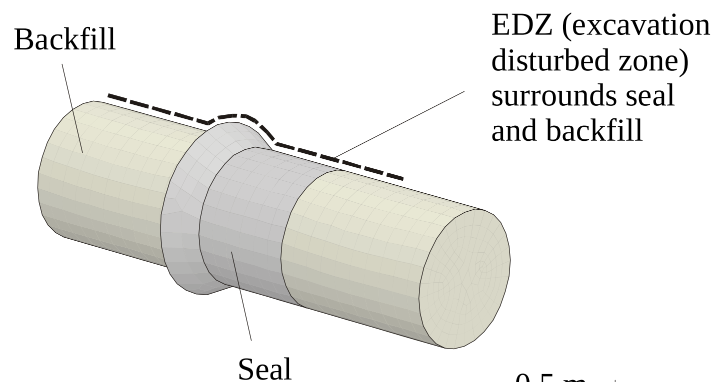

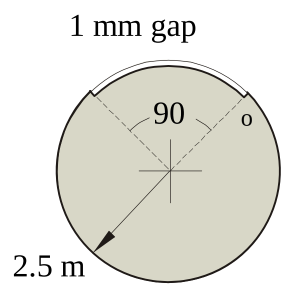

Hydraulic Conductivity

$K_{\text{no gap}} \sim 10^{-9}$ m/s
$K_{\text{1mm gap}} \sim 10^{-3}$ m/s

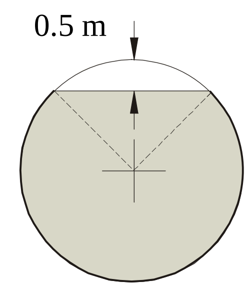

Compaction (6%) due to particle
friction reduction after t~10,000 years

Rock Type	Rock Characteristics				
	Permeability	Ion Exchange	Thermal Conductivity	Strength	Ductility
Clay	Very Low +	Very High +	Low –	Low –	High +
Salt	Impermeable +	None –	High +	Low –	High +
Crystalline	Matrix Low + Fractures High –	Usually None –	Variable o	High +	Low –
Volcanic Tuff	High o	High +	Low –	Low –	Moderate o

Current Research (and Operational) Sites

Clay	Indurated	Bure, France Mont Terri, Switzerland
	Non-Indurated	Benken, Switzerland
Salt	Domal	Mol, Belgium Gorleben, Germany
	Bedded	WIPP, Carlsbad, NM, USA (intermediate level operational)
Crystalline	Unfractured Granite	Pinawa, Manitoba, Canada
	Fractured Granite	Aspö, Sweden, Finland (construction approved May 2002)
Volcanic Tuff		Yucca Mountain, NV, USA (license application construct Dec 2004)

Below water table:
Reducing environment.

Above water table:
Oxidizing environment.

Preferred Respository Host Rocks and Current Research Sites

Some specific issues

- Rock testing (and prediction)

  \- *samples* $\rightarrow$ *coring, slotting*

  \- *full scale* $\rightarrow$ *underground excavations*

- Excavation technology
- Excavation damage
- Time dependent deformation /rock mass strength
- Transparent earth

Unloading path effects on coring, slotting and underground excavation

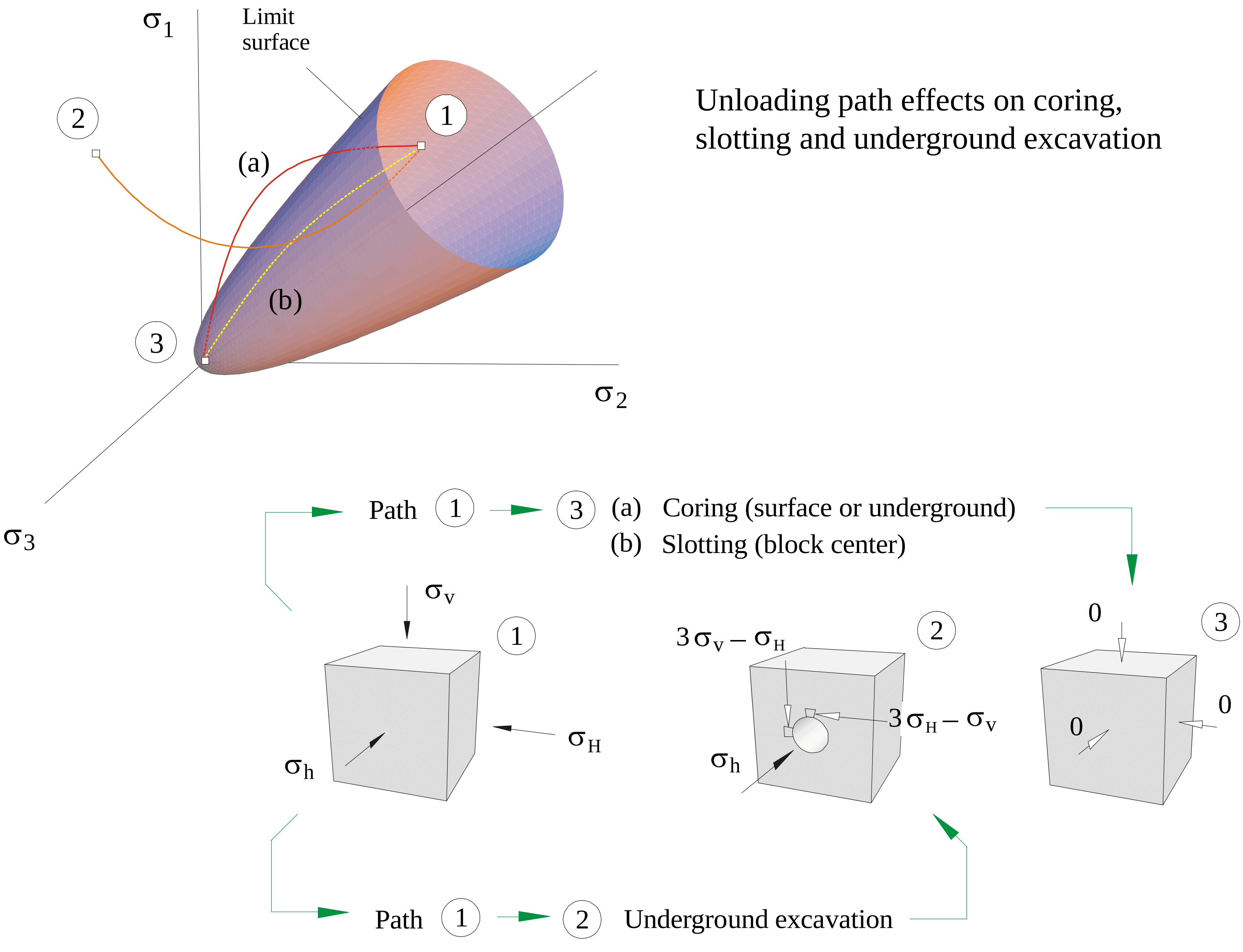

Potential for core damage during coring operation

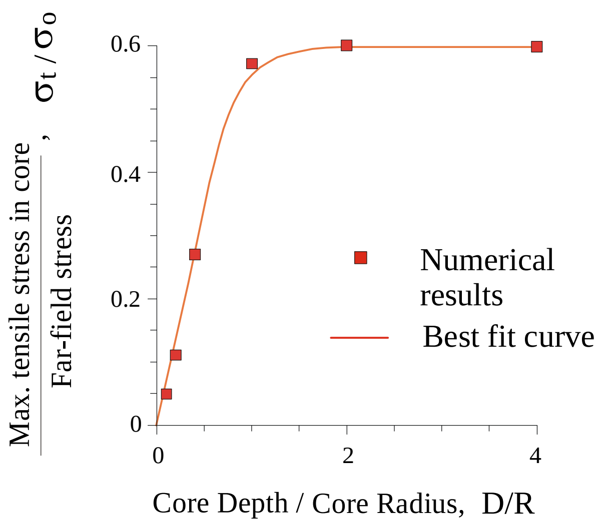

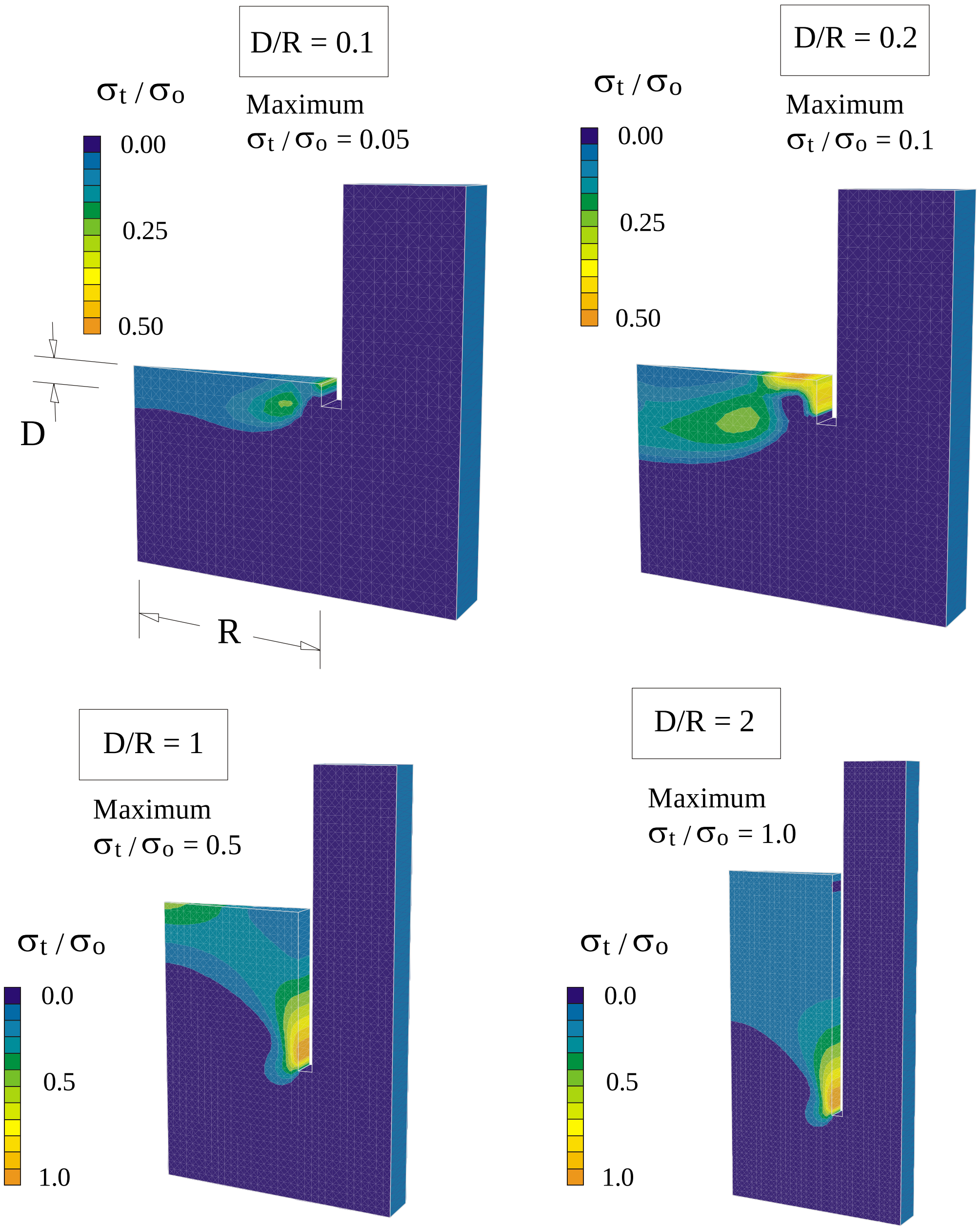

Let $n = \dfrac{\sigma_t}{\sigma_c} = \dfrac{\text{tensile strength}}{\text{compressive strength}}$

[n ~ 0.1]

Let $m = \dfrac{\sigma_t^{\,i}}{\sigma_o} = \dfrac{\text{induced tension in core}}{\text{in-situ horizontal stress}}$

[m ~ 0.5]

<u>Then core damage occurs if</u>

$$\sigma_o > n/m \ \sigma_c$$

i.e., $\underline{\sigma_o > 0.2\ \sigma_c}$

Discing of a 1.3 m diameter core from highly stressed rock (Courtesy of URL/AECL, Canada)

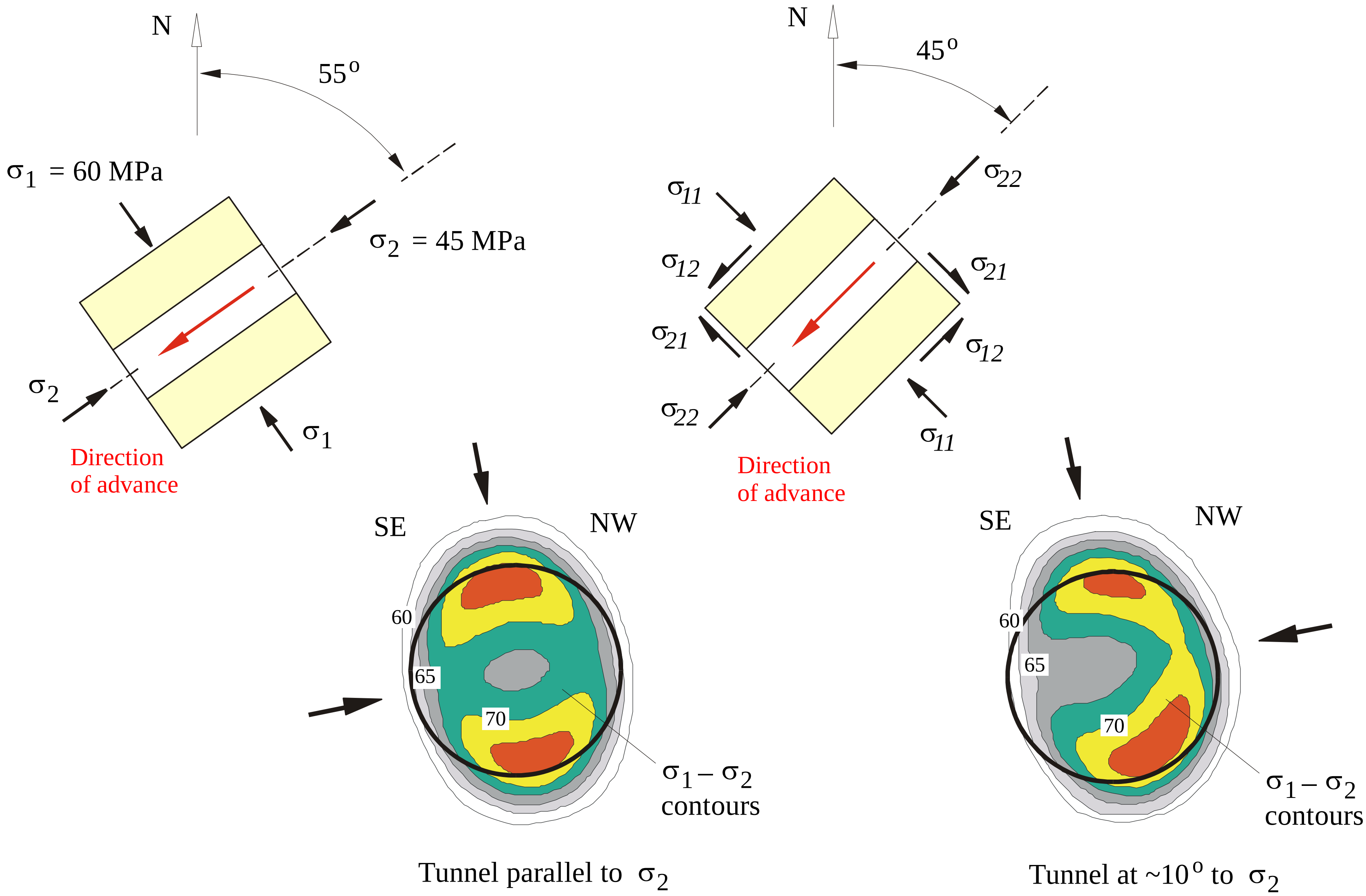

Asymmetric breakout produced by shear stresses acting parallel to excavation (R.S., Read, 1995)

Contours of Maximum Shear Stress $\frac{\sigma_1 - \sigma_3}{\sigma_o}$ developed during slotting of a rock block

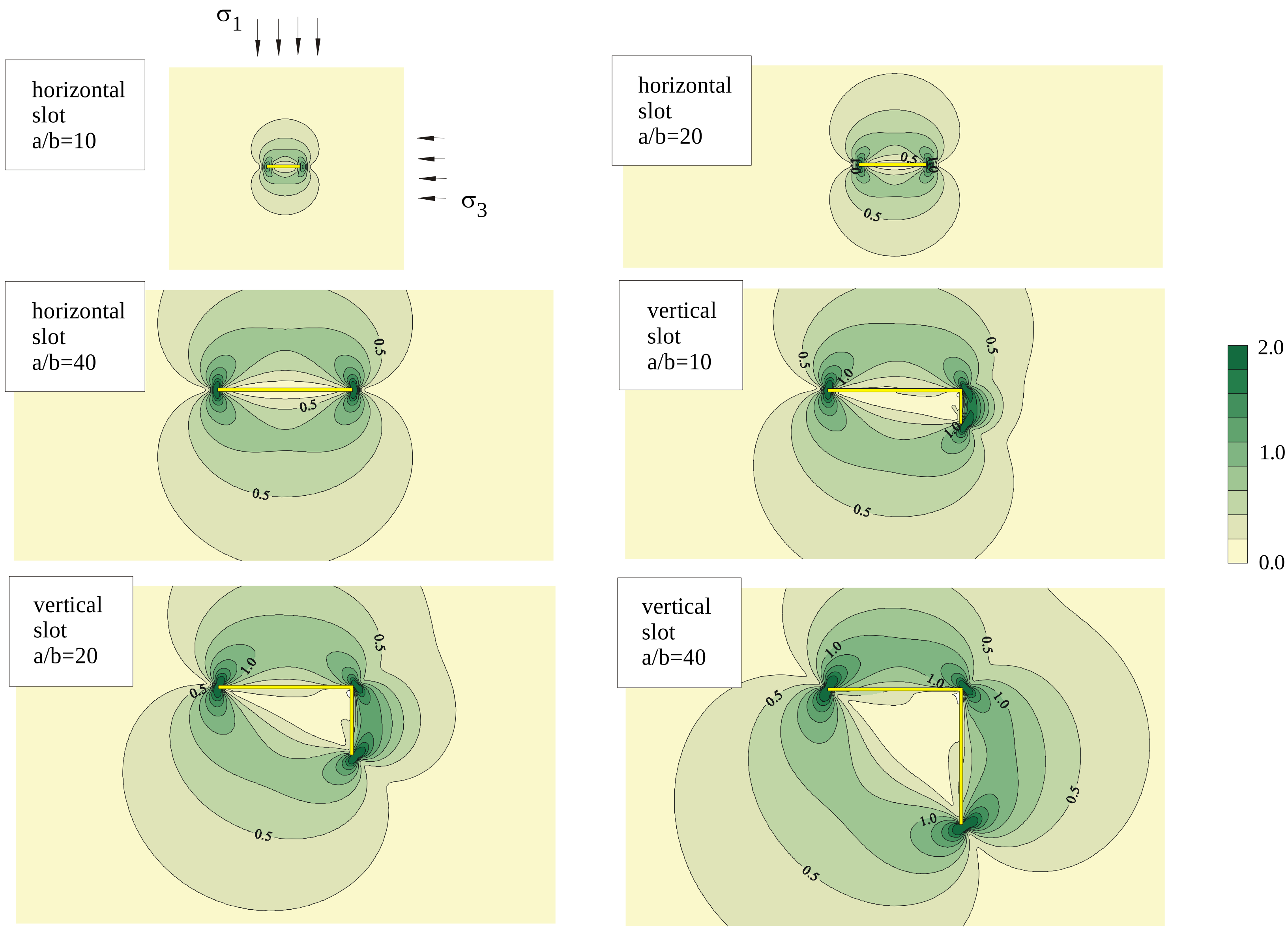

Note: Results are for $\sigma_1 = \sigma_3 = \sigma_o$

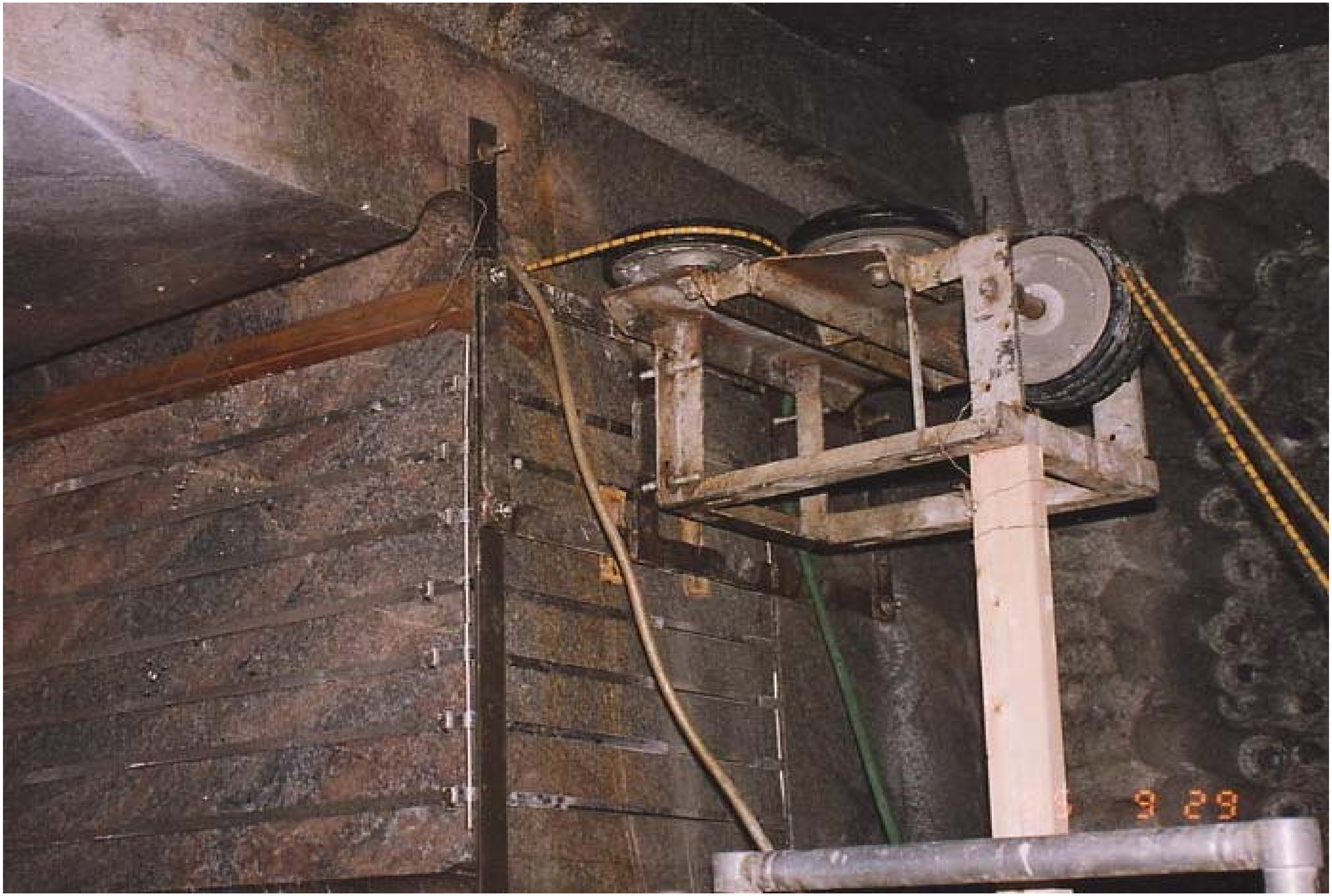

Wire saw slotting tool (Courtesy of URL/AECL, Canada)

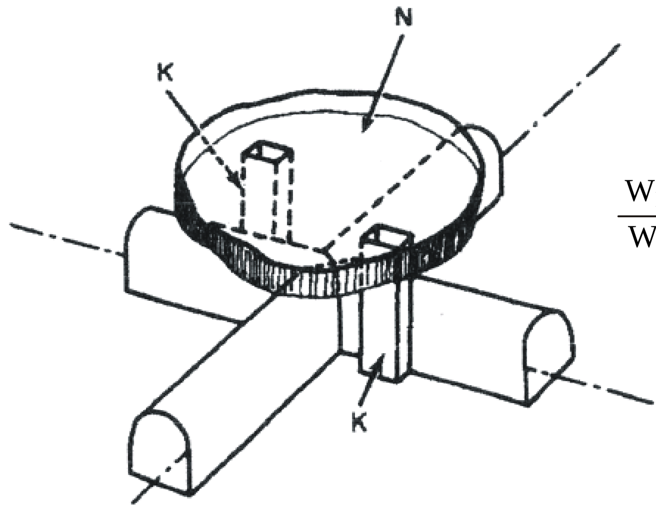

$$\frac{W_N}{W_R} < 1$$

W_N = Stiffness of excavated slot (N)
[slot can be left open or backfilled]

W_R = Rock stiffness

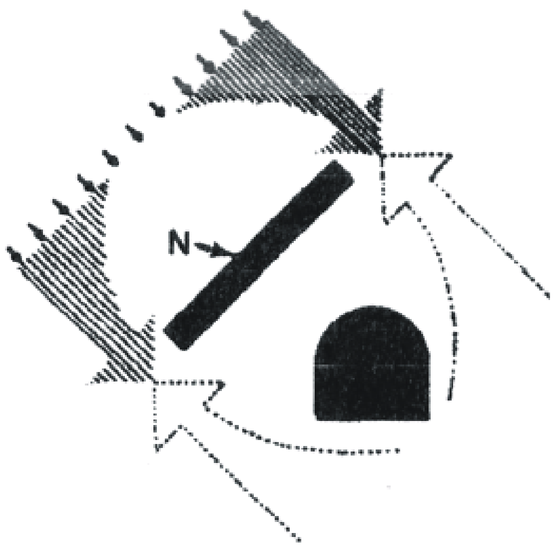

$$\frac{W_N}{W_R} < 1$$

$$\frac{W_N}{W_R} < 1$$

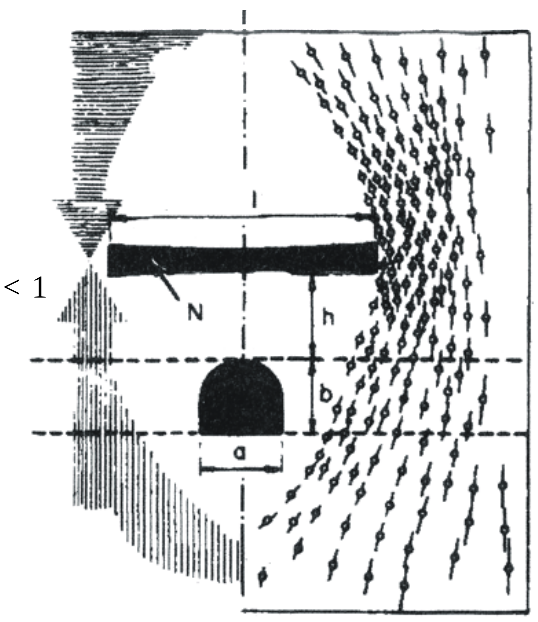

Slotting technique proposed by Kvapil (1962) to increase the stability of 'critical' underground excavations (e.g., intersections) in highly stressed rock.

Tunnel Near-field. Disintegration of EDZ

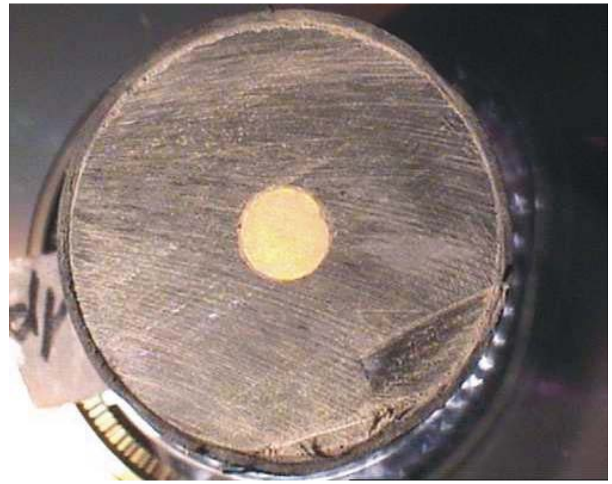

σ_c = 13 MPa
water circulated in inner borehole

σ_c = 30 MPa
dry inner borehole

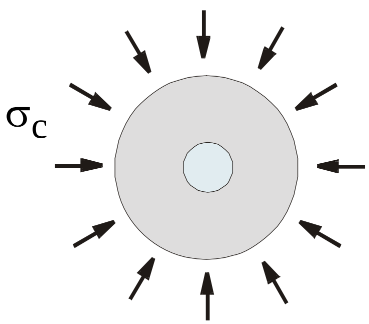

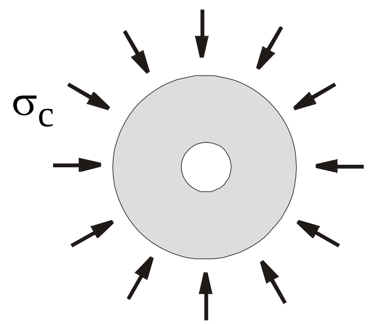

Effect of water on the EDZ in the Opalinus Clay, Mont Terri, Switzerland (Courtesy of nagra)

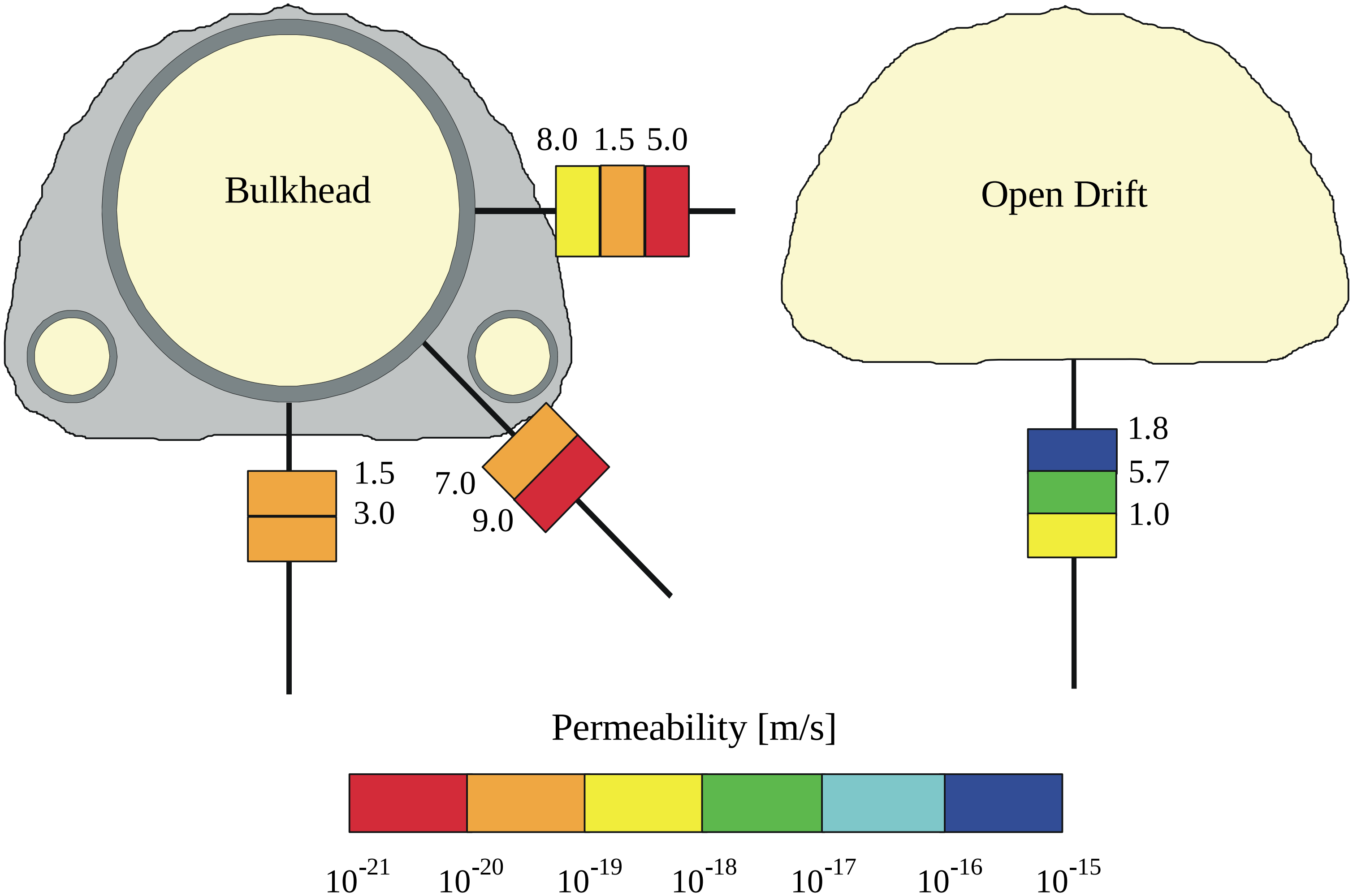

ALOHA2: Permeability Distribution Around the Bulkhead Drift (Courtesy of GRS)

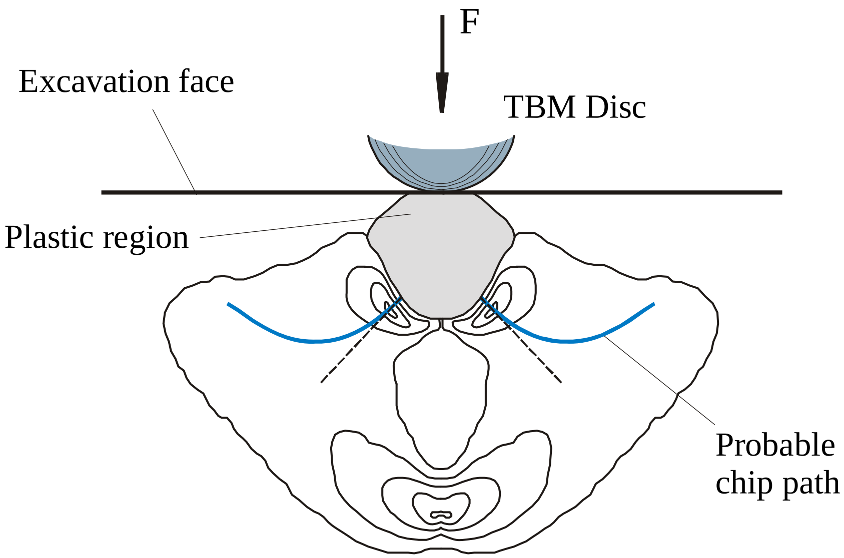

Stress distribution beneath a TBM Disc Indenter
after the stable vertical crack has developed

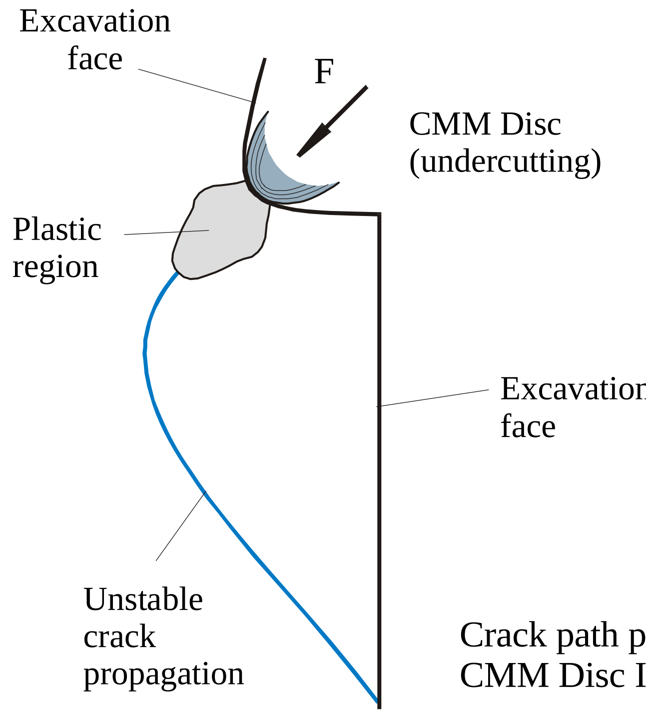

Crack path produced by
CMM Disc Indenter

Note: Tensile crack can not propagate
until plastic region reaches critical size

Disc tip radius	CMM Indenter Force (N/mm of contact length)			
	S = 25 mm	S = 50 mm	S = 100 mm	S = ∞
6 mm	1,700 (74%)	2,310 (100%)	2,700 (117%)	3,000 (130%)
8 mm		2,500 (100%)	3,150 (126%)	(3,500?) (140%?)
12 mm		3,150 (100%)	3,600 (114%)	4,200 (133%)

Note: Indenter Force Increase is small for large increase in cutting depth S.

Comparison of chip formation in classical TBM and in CMM (undercutting)

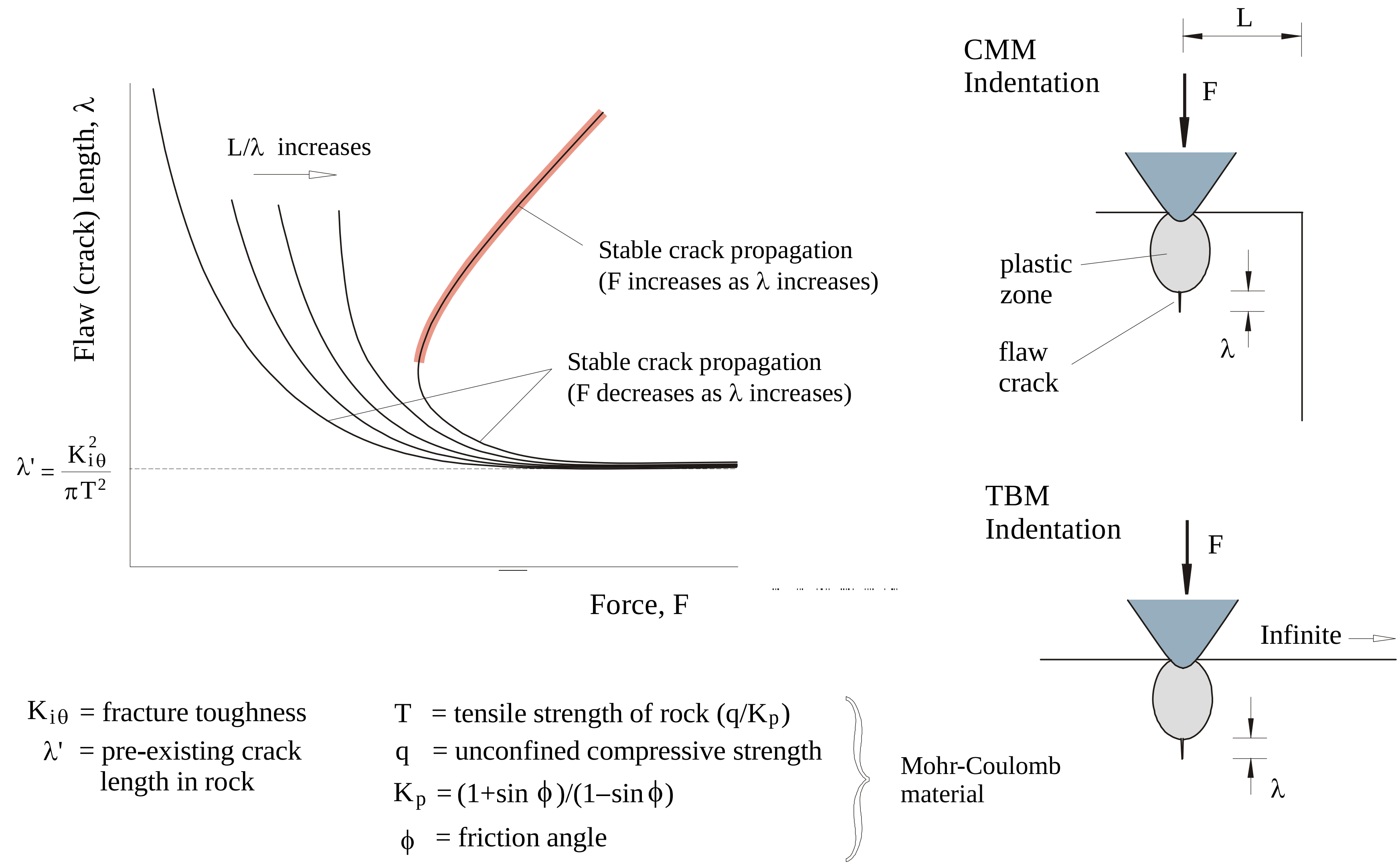

Relationship between applied force on an indenter and the length of edge crack (λ) beneath the plastic crushed zone

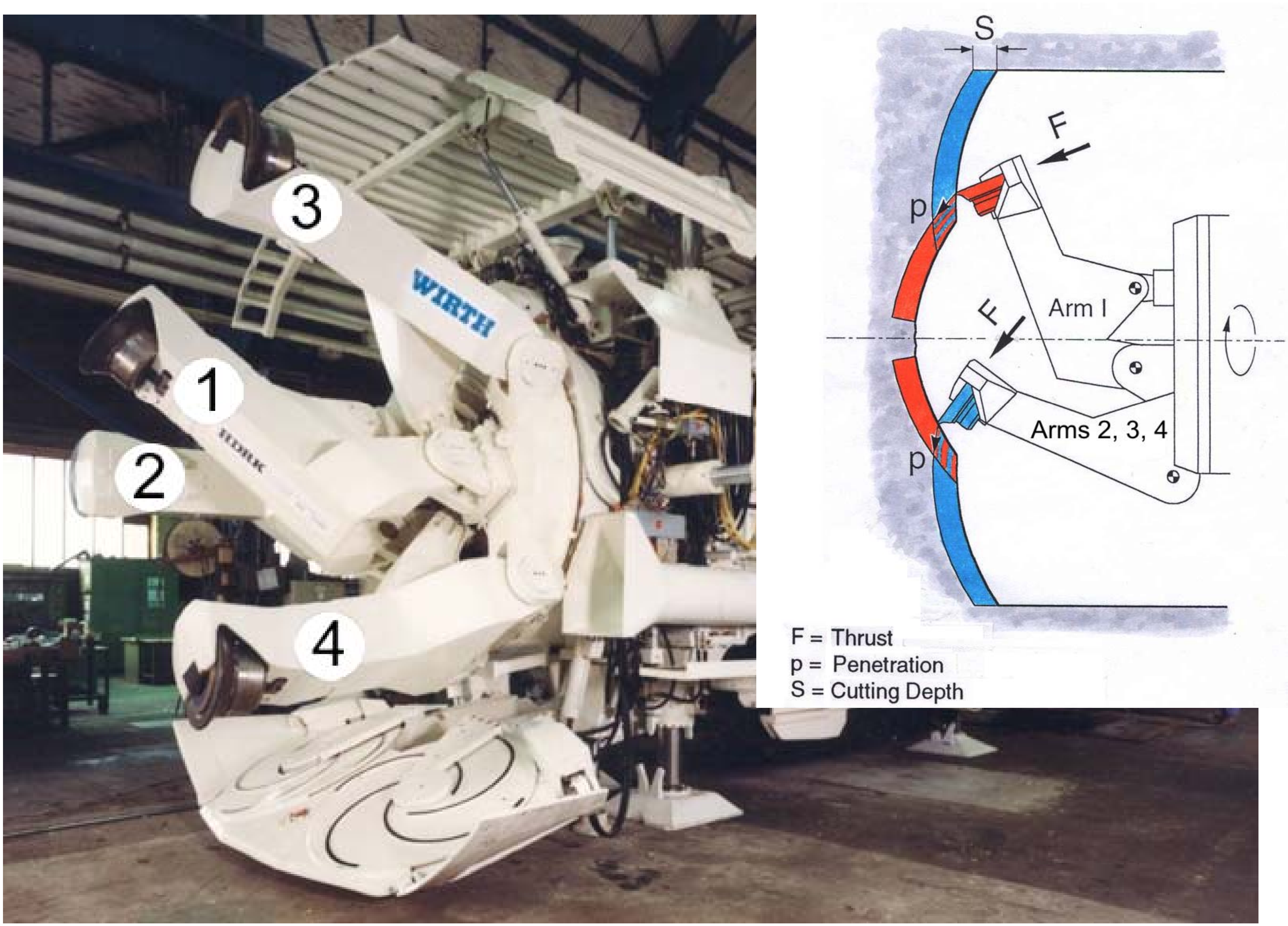

WIRTH-HDRK Continuous Mining Machine (CMM)

Rock cuttings produced by CMM

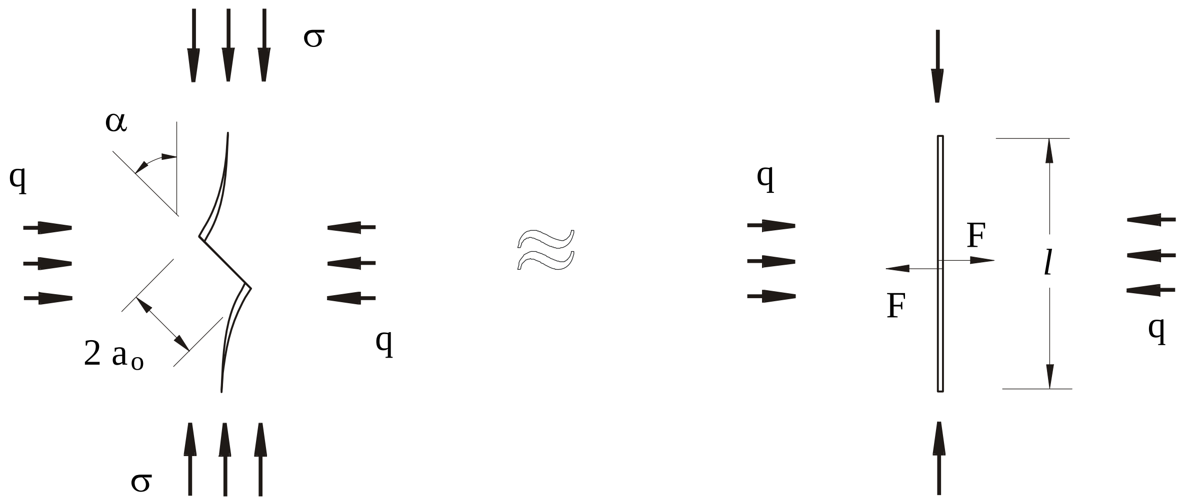

Wing crack growth under compression, Fairhurst and Cook (1966) model

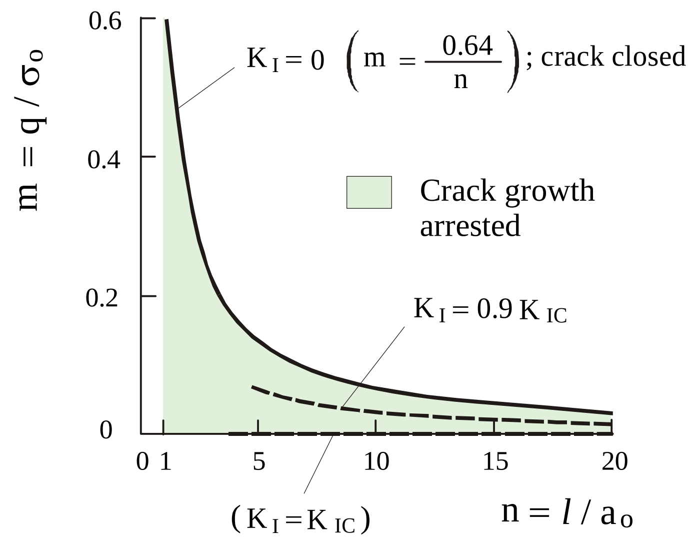

$$K_I = F / \sqrt{\pi l} - q\sqrt{\pi l}\ ; \qquad F = 2\sigma\, a_o \qquad (1)$$

Crack growth if $K_I > K_{IC}$ $[\sigma > \sigma_c]$

(after Germanovich and Dyskin, 2000)

Rewriting (1)

$$K_I = \sigma_o \sqrt{a_o}\left[\frac{2}{\sqrt{n\pi}} - m\sqrt{n\pi}\right]$$

where $n = l / a_o$ $\qquad m = q / \sigma_o$

$$K_I = 0 \quad \text{if} \quad m \geqslant \frac{2}{n\pi} \simeq \frac{0.64}{n}$$

Supression of crack growth by small confining pressure

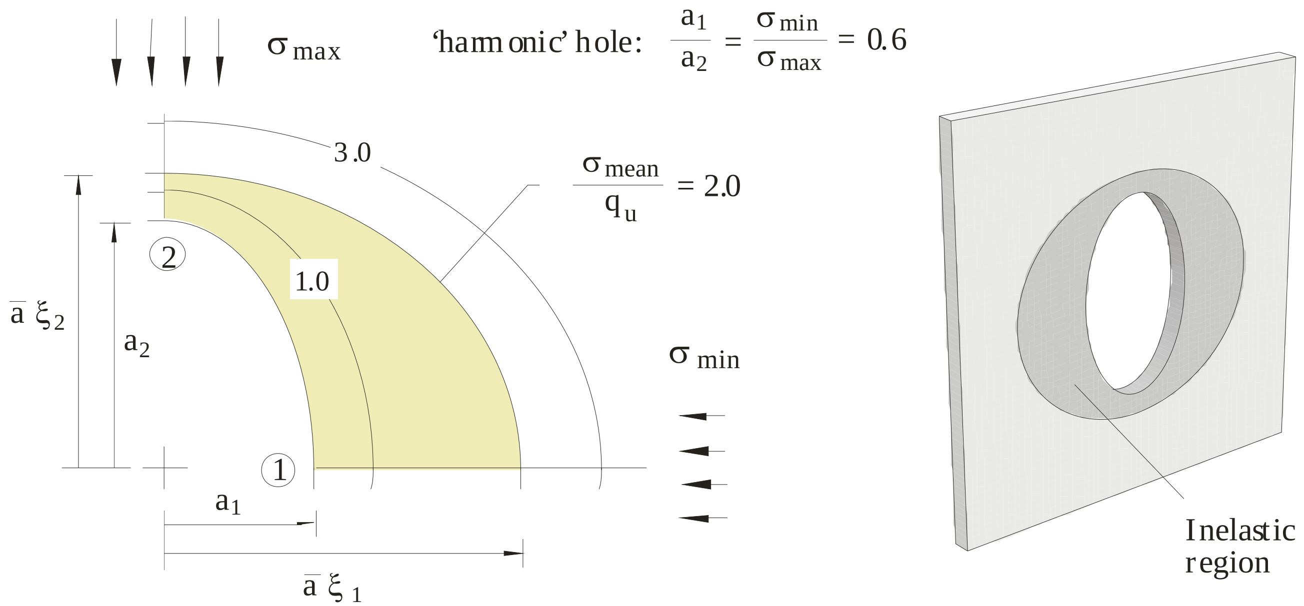

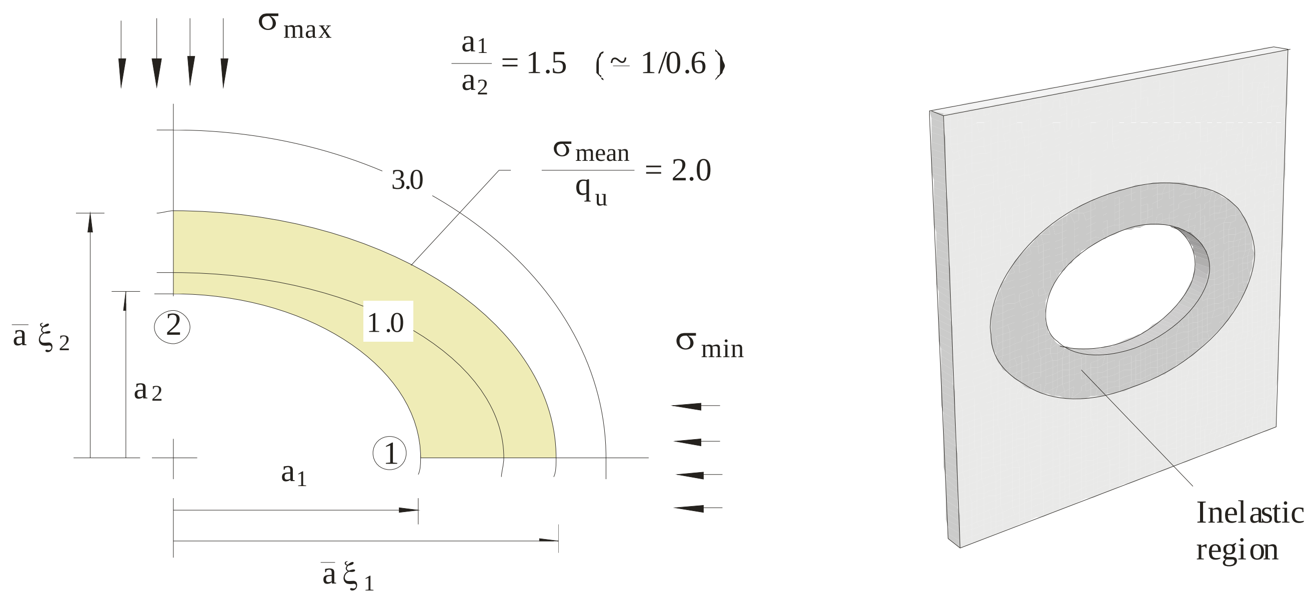

"Harmonic Hole" —Optimum shape of hole to minimize the extent of excavation damage?

$$\frac{a_1}{a_2} = \frac{\sigma_{min}}{\sigma_{max}} = 0.6$$

$a_1 = 1.2$ m $\quad \sigma_{min} = 1.19$ MPa

$a_2 = 2.0$ m $\quad \sigma_{max} = 0.71$ MPa

Thermal properties

$\kappa = 3$ W/m^{o}C

$c_p = 844.83$ J/kg^{o}C

$\alpha_t = 40 \times 10^{-6}$ 1/^{o}C

Mechanical properties

$\phi = 30^o$

$q_u = 1$ MPa

$\rho = 2650$ kg/m^3

Wall temperature T=100^{o}C
(fixed)

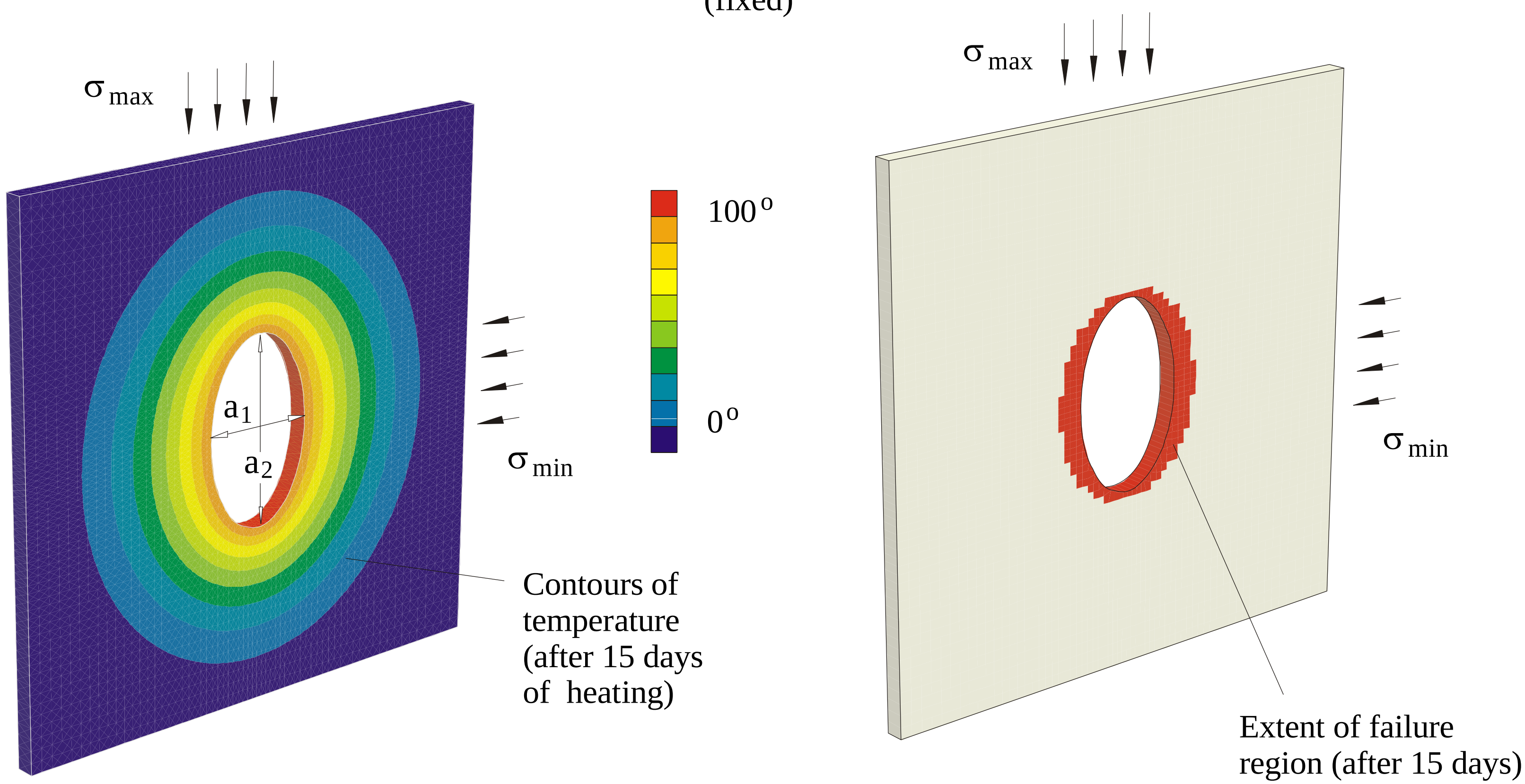

"Harmonic Hole" —Effect of thermal load on excavation damage

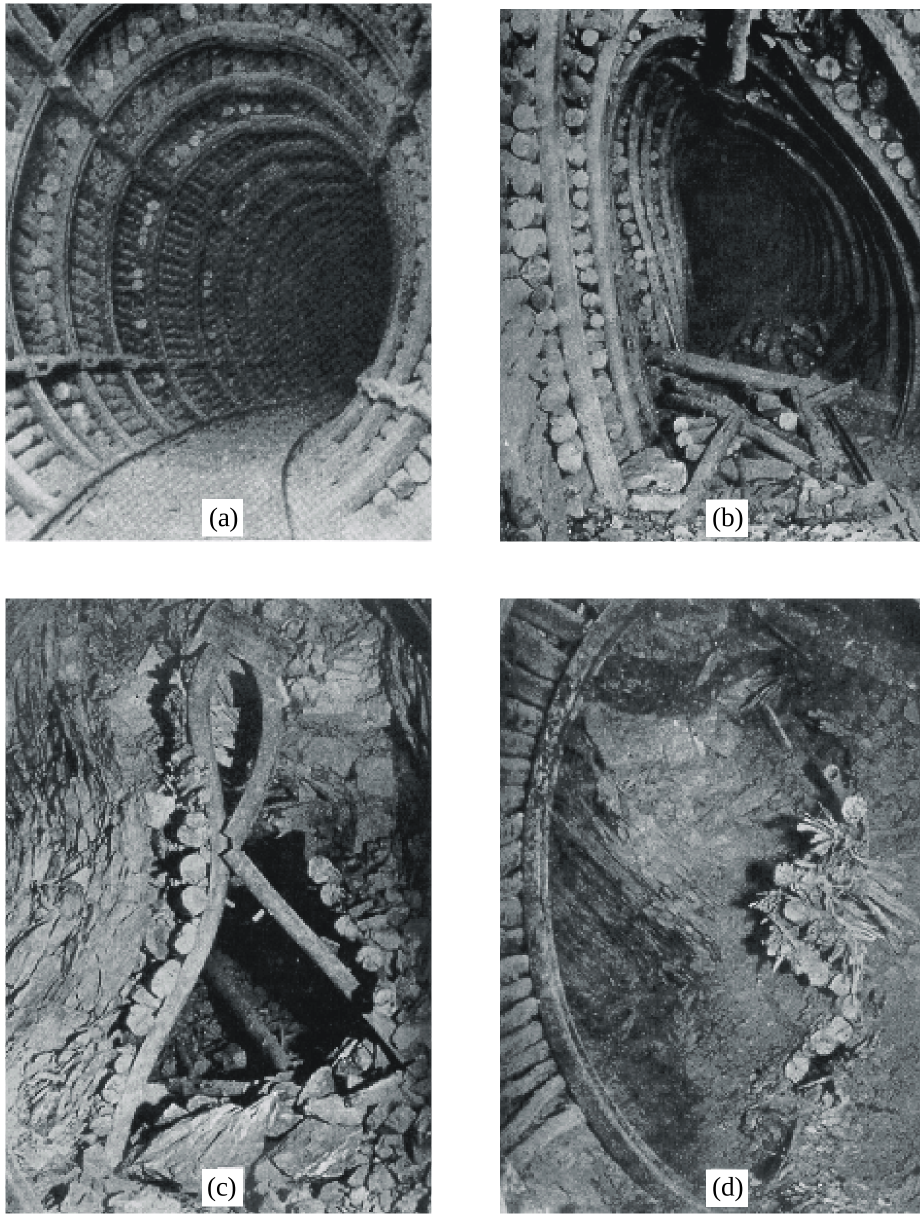

"Harmonic hole" - Kolar Gold Fied (Caw, 1956) a)

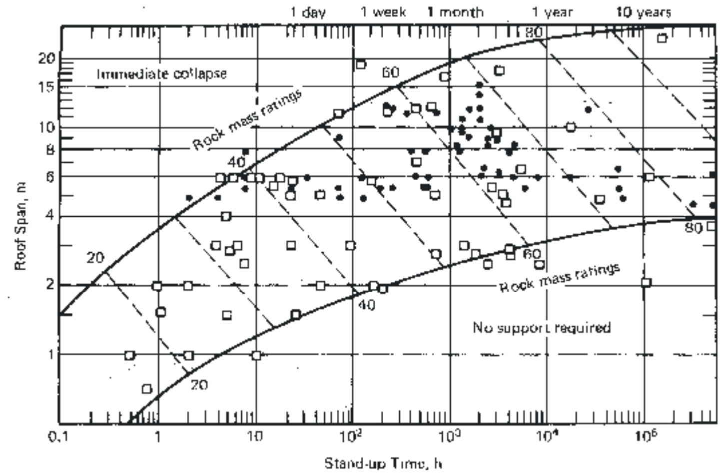

b)

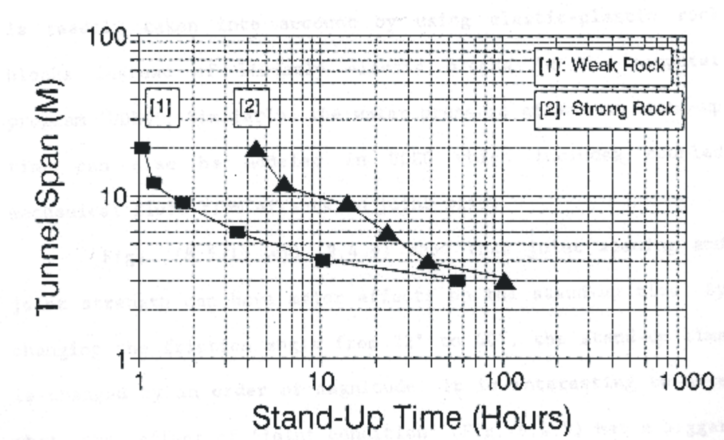

(a) Empirical stand-up time relations for tunnels as a function of span and rock quality defined by the Rock Mass Rating System; (b) Theoretical stand-up time based on joint strength deterioration with time (after Fakhimi 1992).

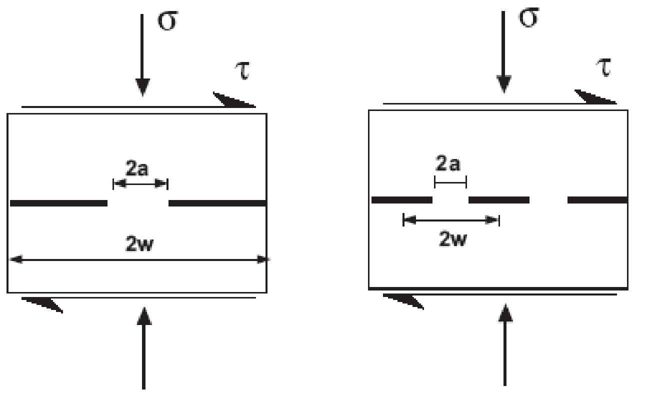

Fracture mechanics models, a) single rock bridge under far field normal and shear stresses; b) multiple rock bridge under far field normal and shear stresses.

$$C_0 = \frac{\sqrt{\pi}\left[a_o^{1+n/2} - \left(1+\frac{n}{2}\right)At\left[\frac{2w(\tau - \sigma_n \tan\phi)}{K_{IIC}\sqrt{\pi}}\right]^n\right]^{1/(2+n)}}{2w}$$

$$FS = \frac{C_0 + \frac{W}{A_s}\cos\theta\tan\phi}{\frac{W}{A_s}\sin\theta}.$$

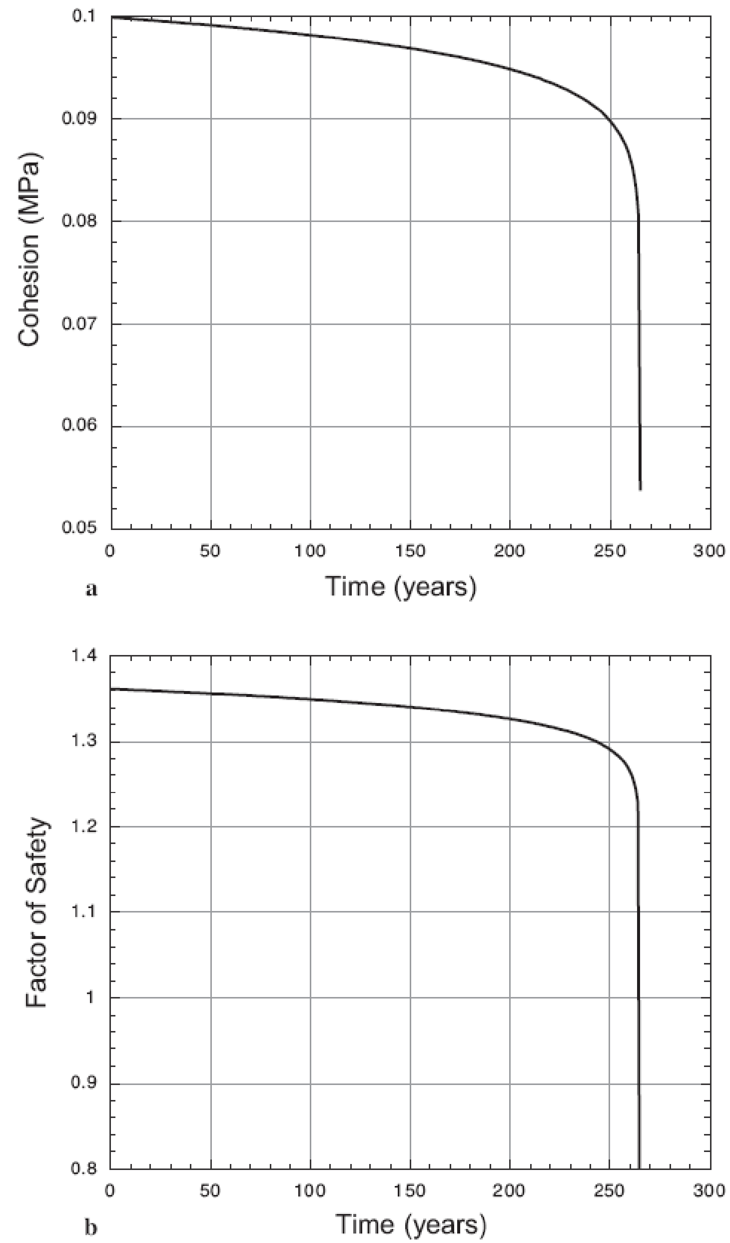

Cohesion and safety factor as a function of time.

From Kemeny, 2003

Linear contact law

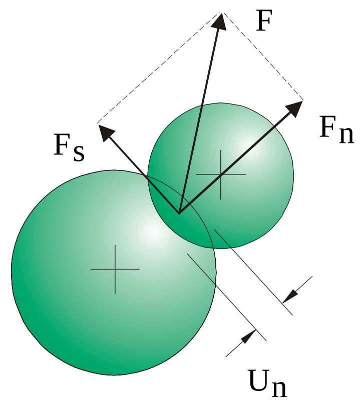

Contact law

$$F_n = K_n \cdot U_n$$
$$\Delta F_s = K_s \cdot \Delta U_s$$

Slip condition

$$F_s = \mu F_n$$

Deformation is assumed to occur at contact point only.

Constitutive behavior at contact between two particles

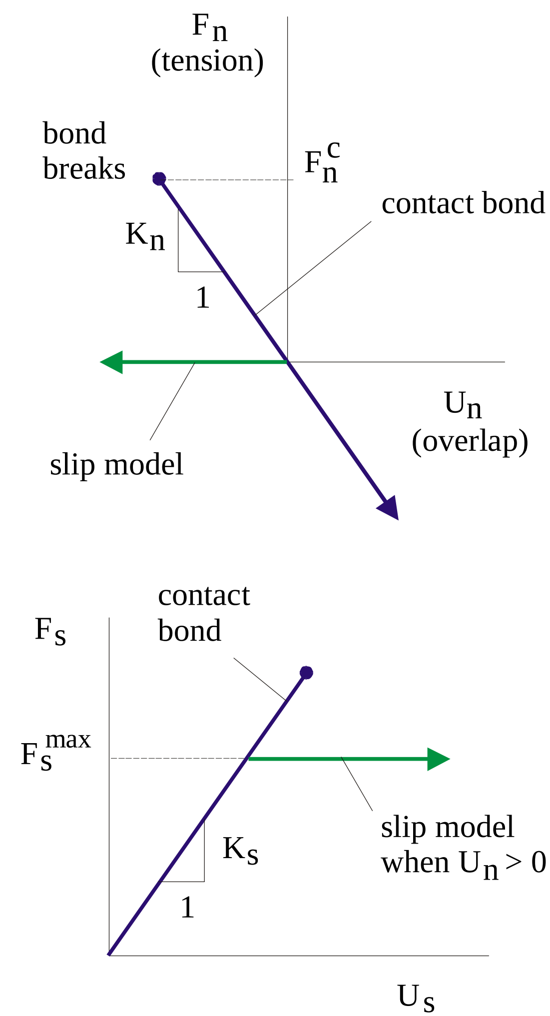

Contact bond

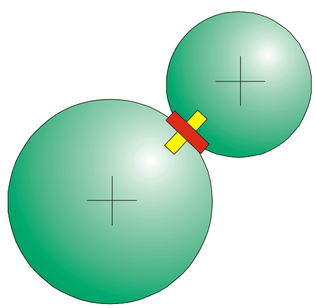

Models adhesion over vanishingly small area of contact point (does not resists bending moment); breaks if normal or shear force exceeds bond strength.

Parallel bond

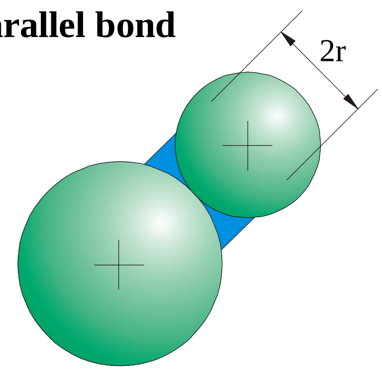

Models additional material deposited after particles are in contact (resists bending moment); breaks if normal or shear stress exceeds bond strength.

Particulate mechanics (PFC -Cundall and Potyondy)

Parallel-bonded stress corrosion model

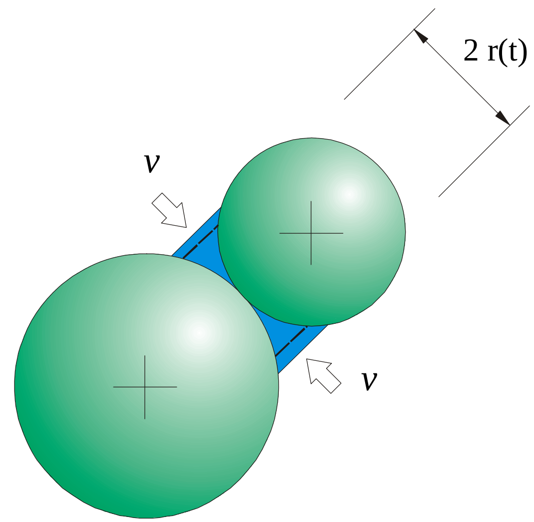

- Stress-dependent corrosion reaction occurs at micro-tension sites.

  Corrosion reaction occurs at the periphery of parallel bonds and removes bond material

- Reaction rate is determined by local driving force and local energy barrier.

  1) Driving force: bond stress (sigma)

  2) Energy barrier: micro-activation stress (sigma_a)

- Express corrosive-front velocity as:

$$v = \beta_1 e^{\beta_2 (\bar{\sigma} / \bar{\sigma}_c)}$$

$v = 0$ if sigma < sigma_a

PFC simulation of time dependent weakening of rock

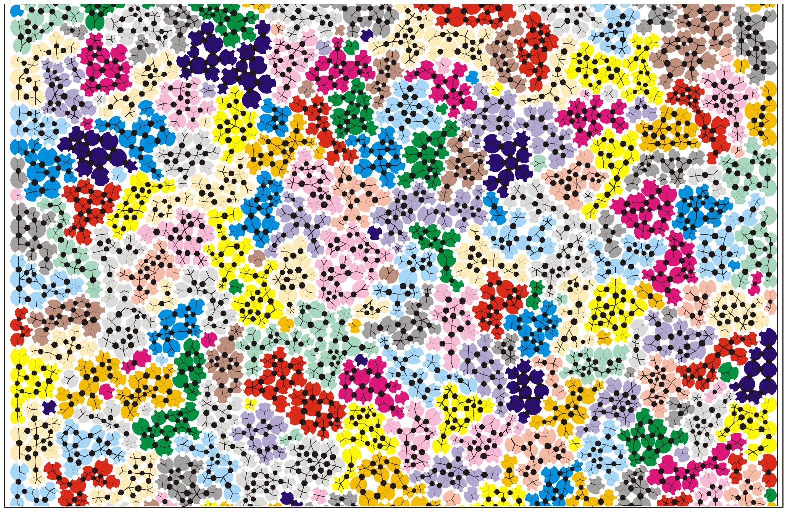

Cluster of particles

Compression test on assembly of particles

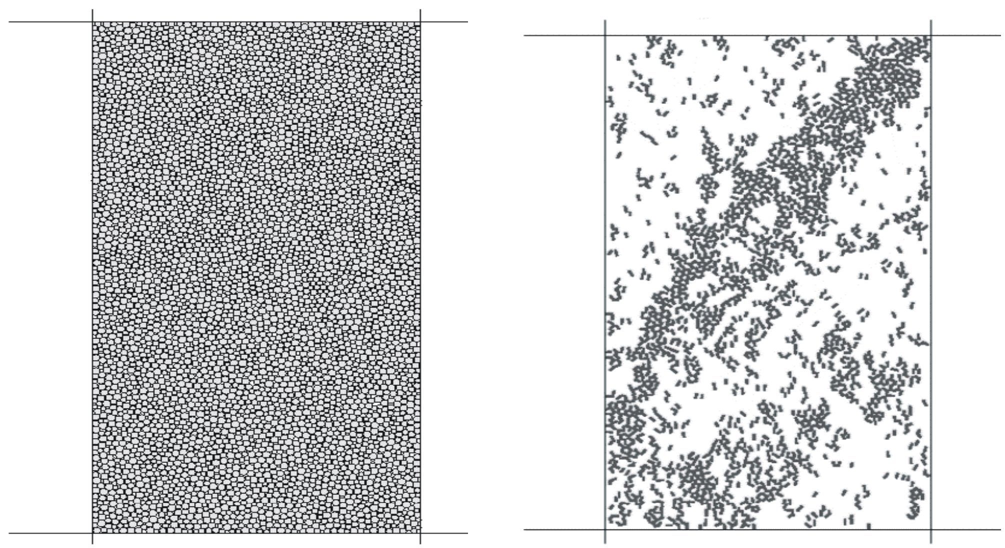

PFC model of a particulate assembly (rock) and compression loading

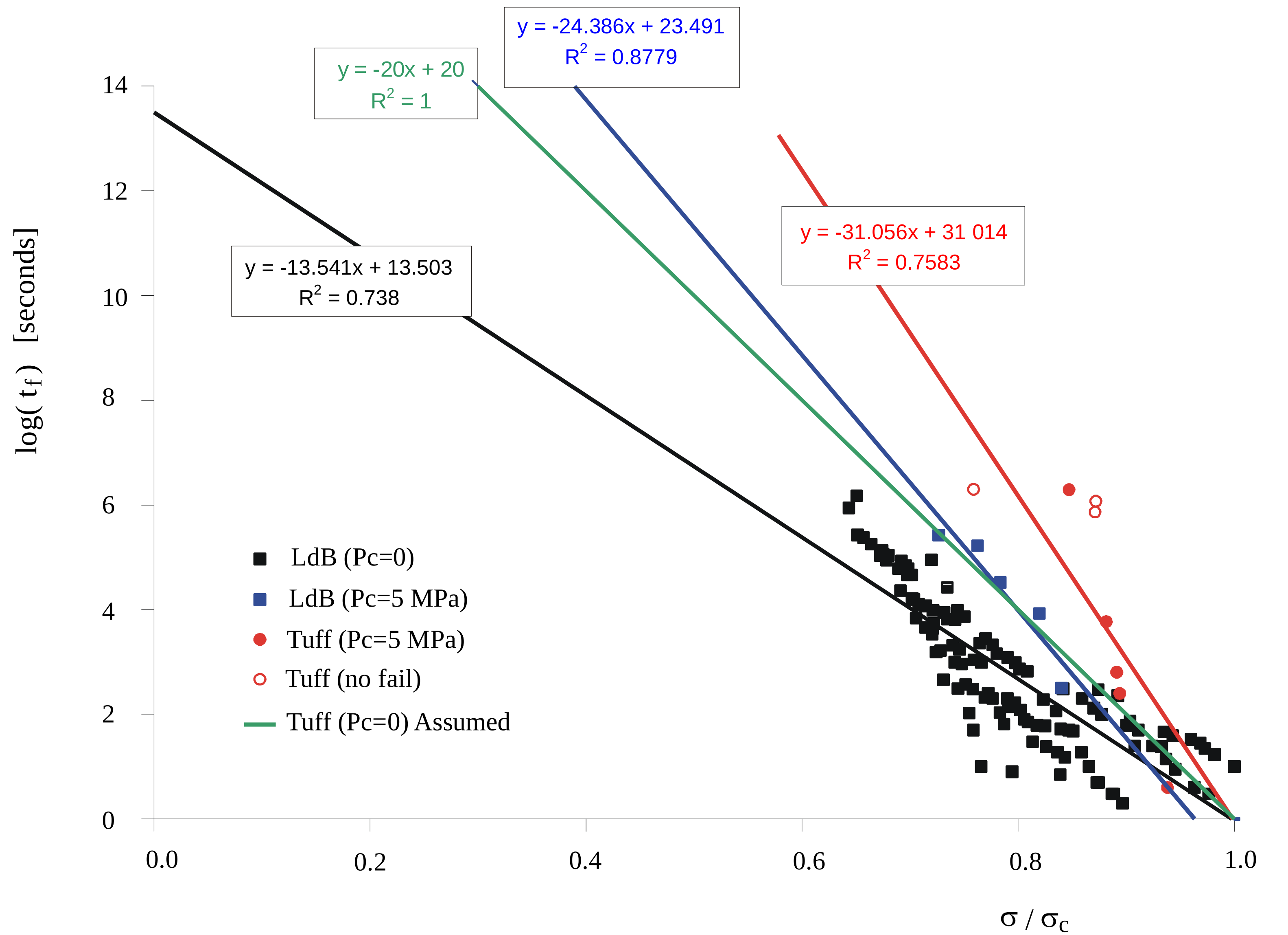

Static Fatigure Curves used as input to the UDEC analysis of collapse over time at Yucca Mountain

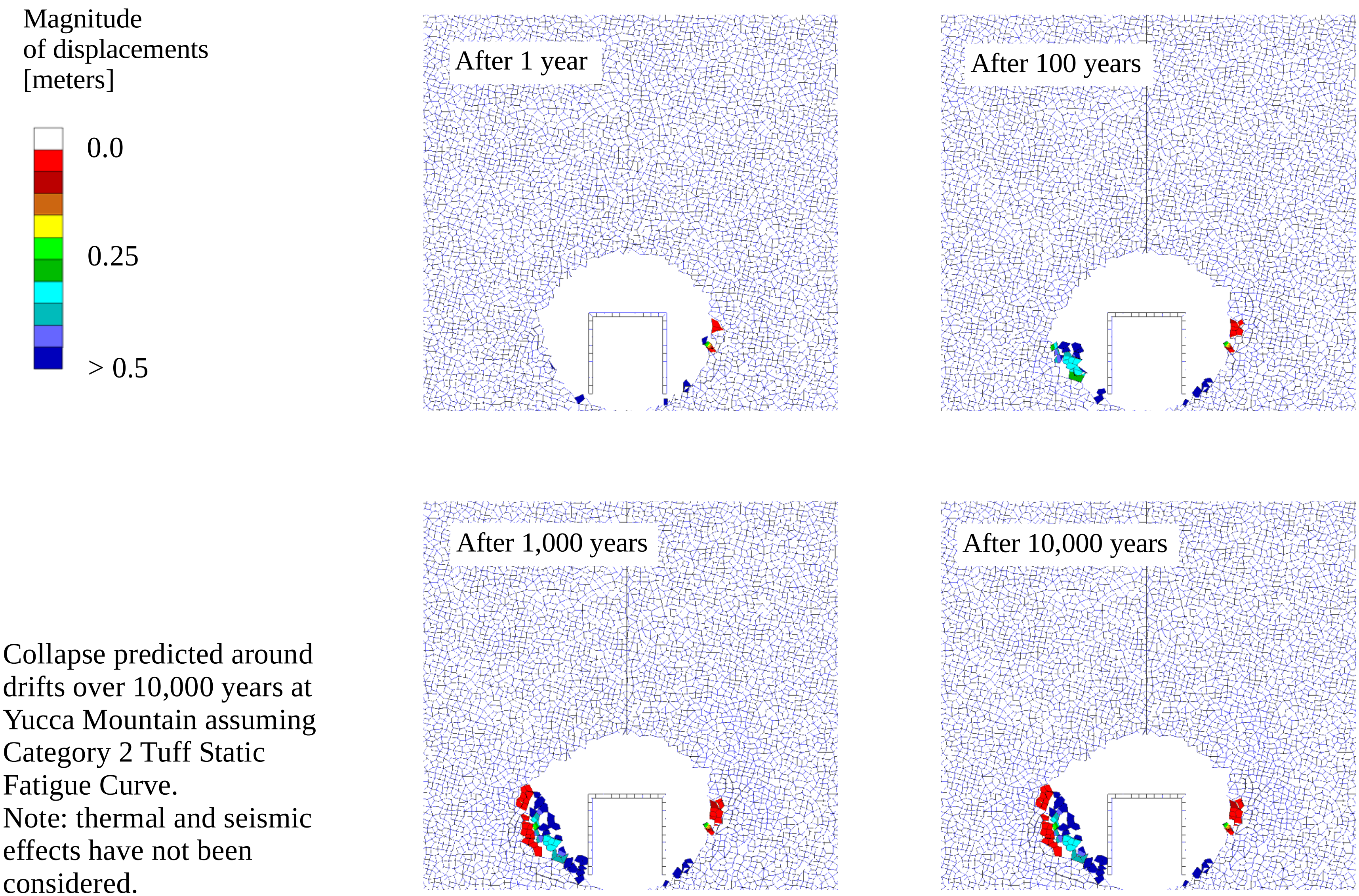

Collapse predicted around drifts over 10,000 years at Yucca Mountain assuming Category 2 Tuff Static Fatigue Curve.
Note: thermal and seismic effects have not been considered.

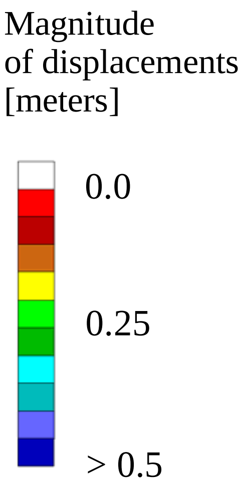

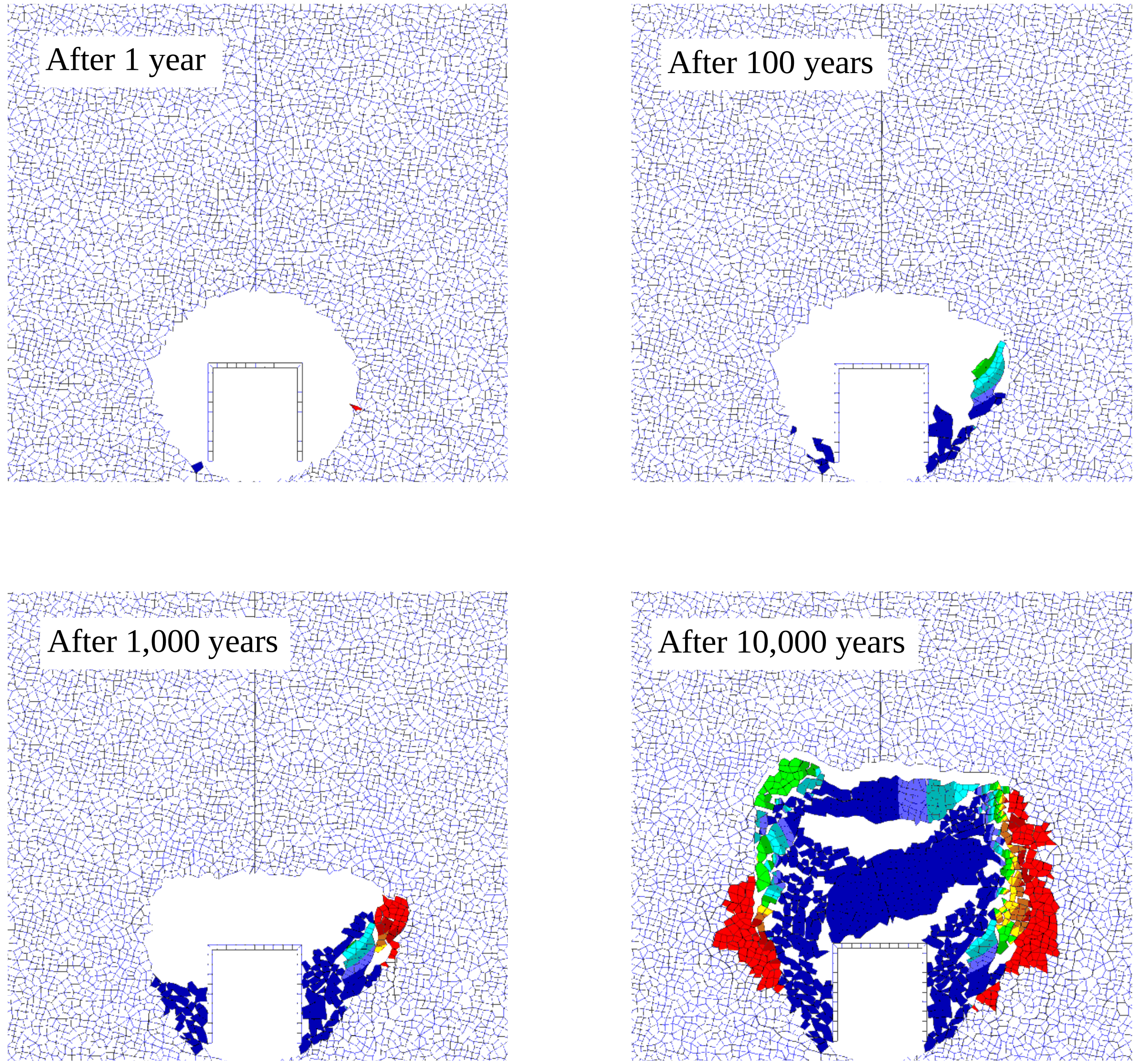

Collapse predicted around drifts over 10,000 years at Yucca Mountain assuming Category 2 Lac du Bonnet Static Fatigue Curve. Note: thermal and seismic effects have not been considered.

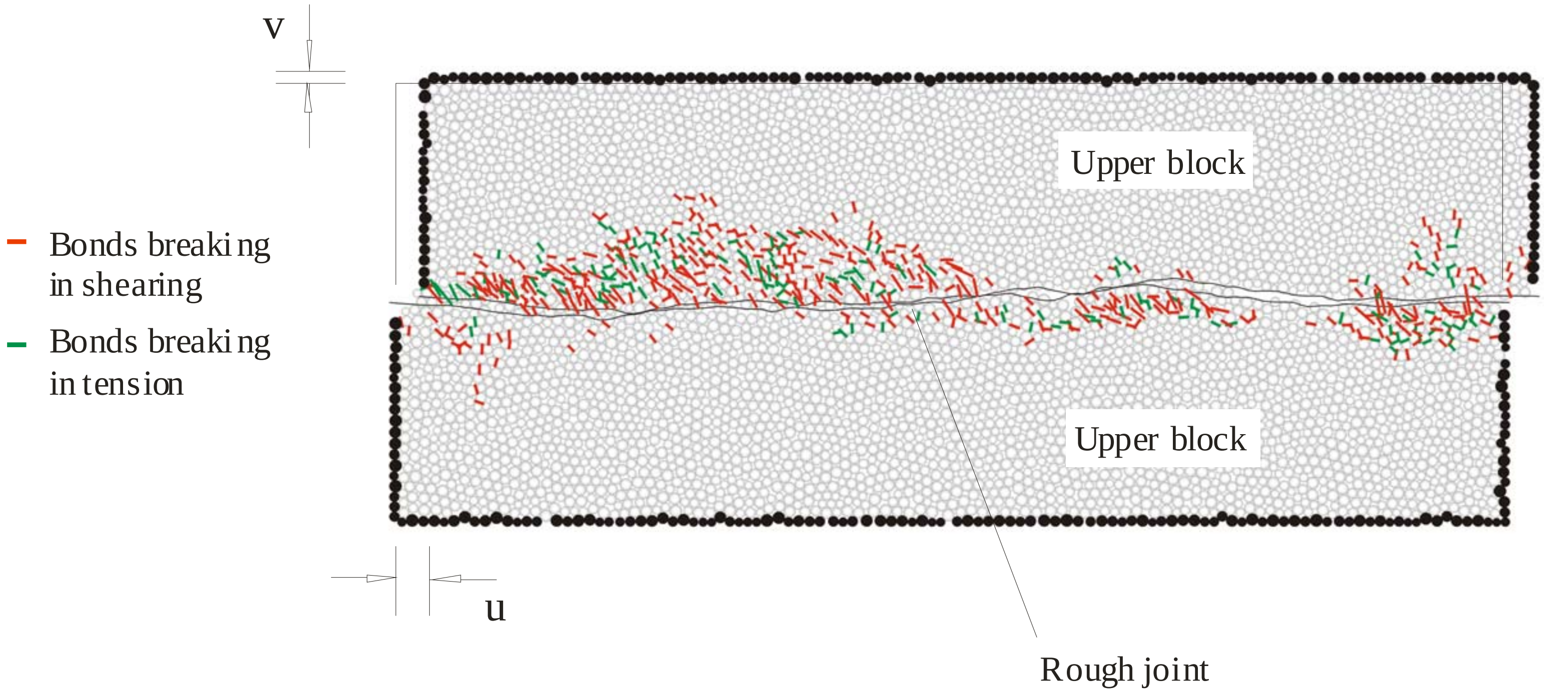

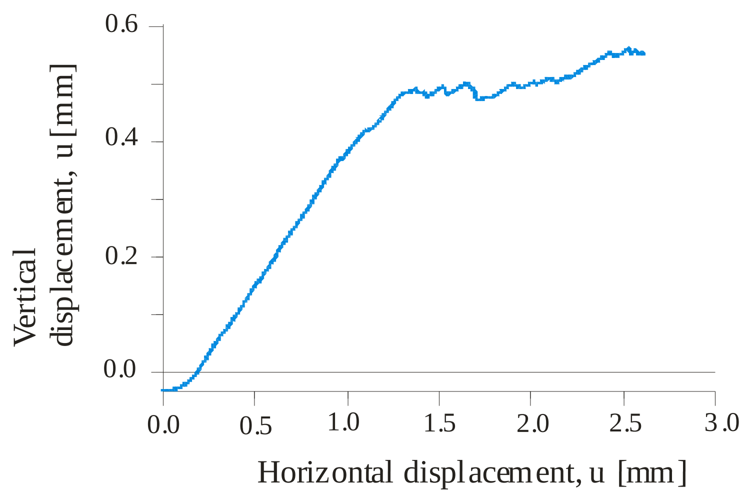

Dilation response of the joint sample as measured during the PFC shearing experiment (no relative rotation of upper and lower blocks allowed)

Use of PFC to examine the shear behavior of a rough joint.

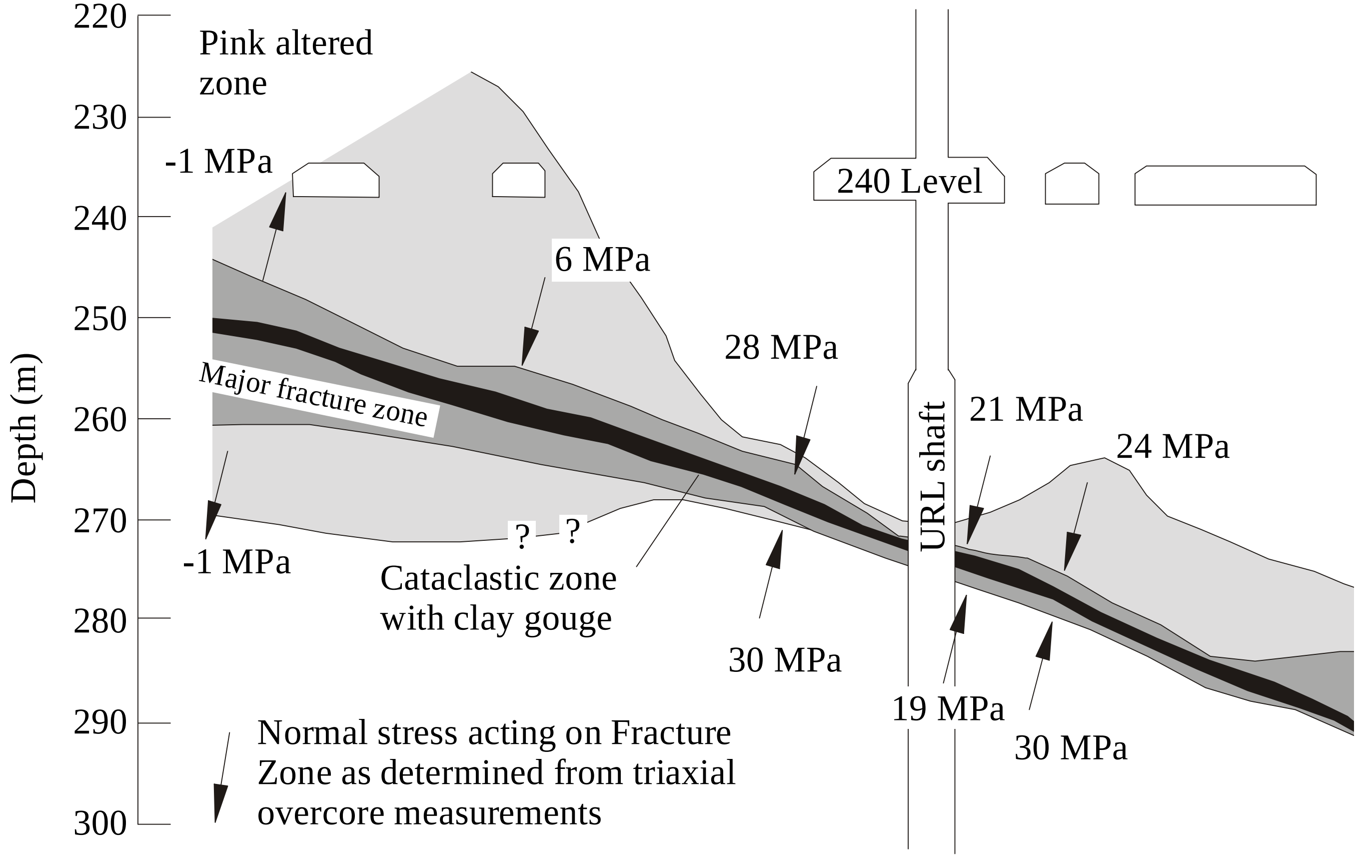

Observed variability of normal stress across a thrust fault at the URL, Pinawa,Canada.

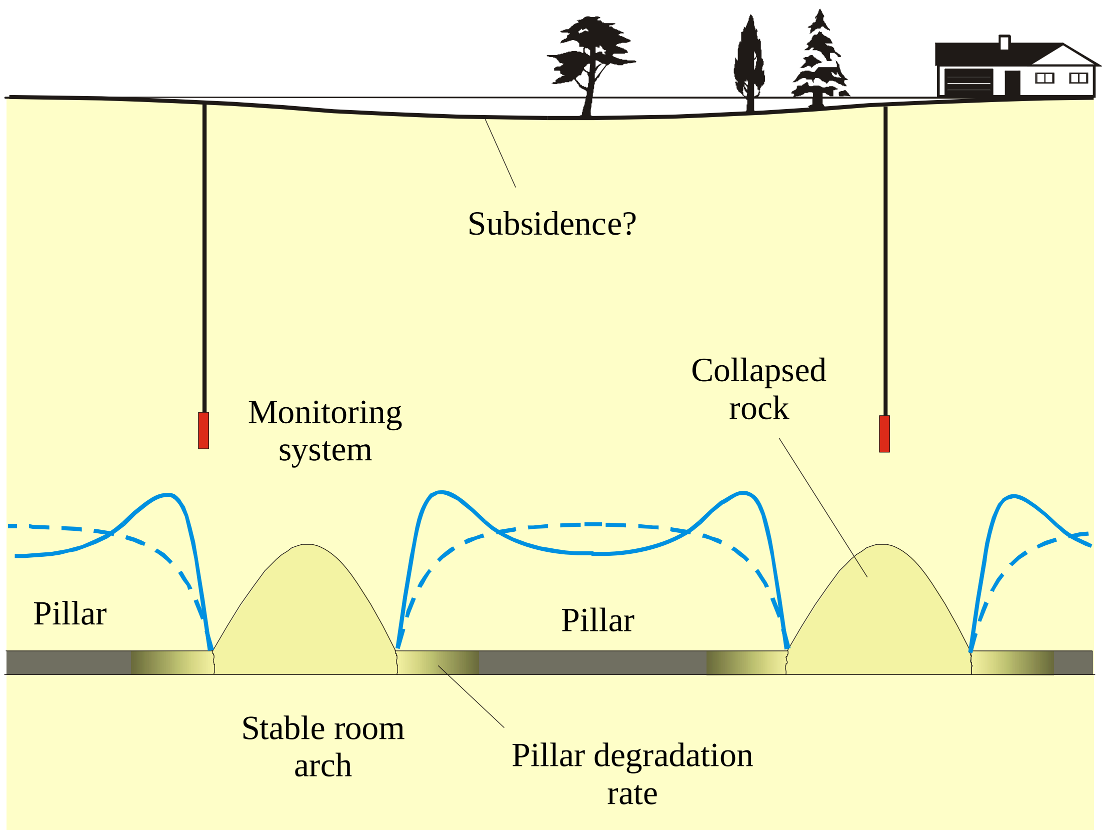

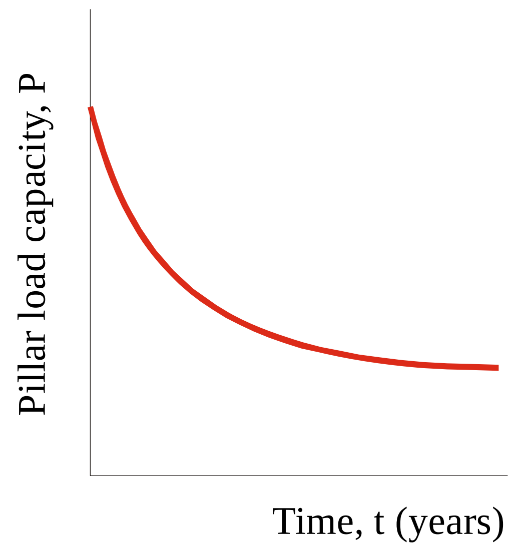

Prediction of long-term (50~100 yr) behaviour of Pillars and Large Excavations in abandoned mines

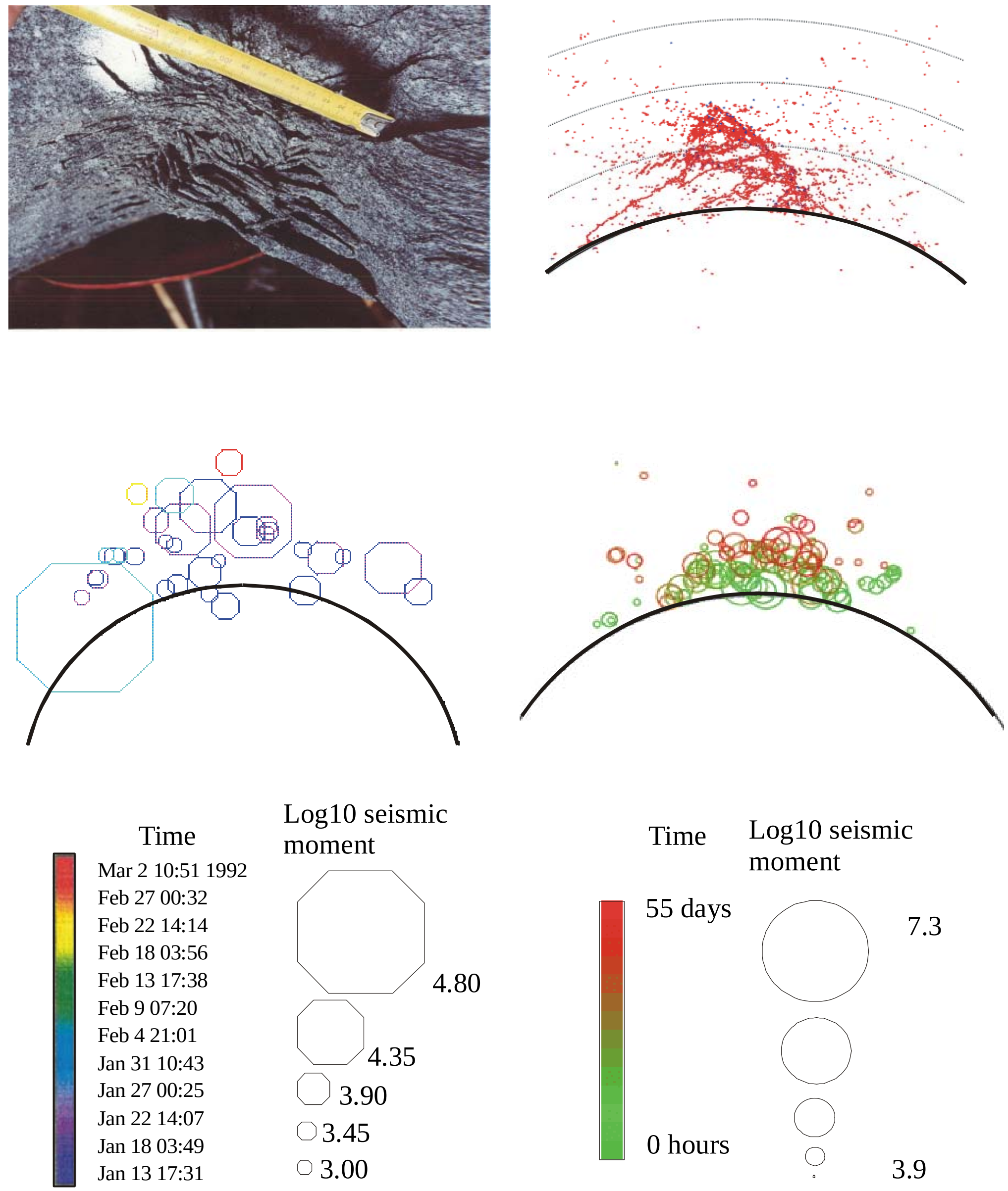

Breakout PFC analysis

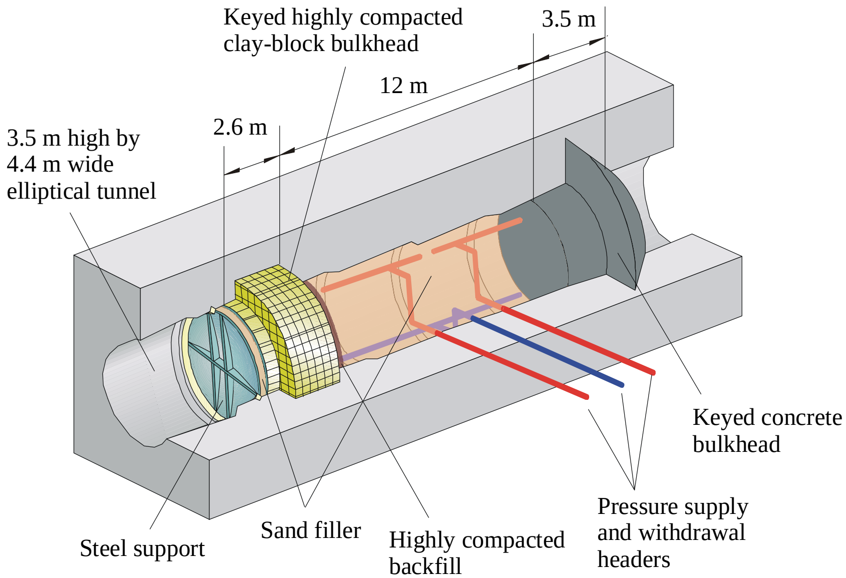

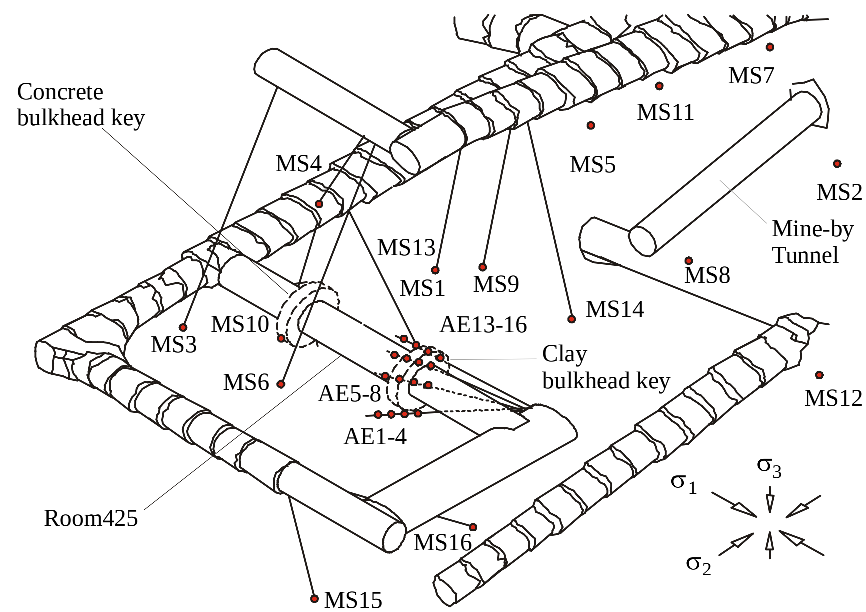

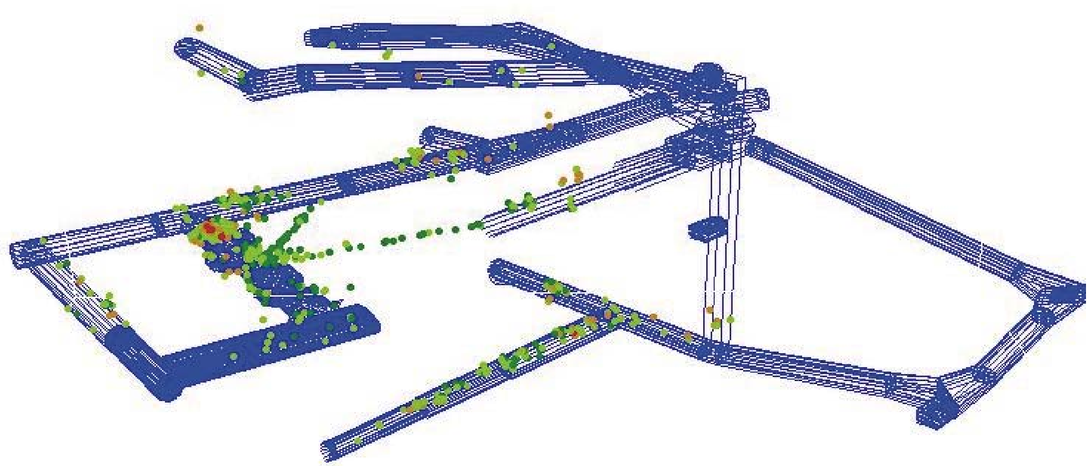

Transparent Earth. URL TSX AE (Courtesy of Professor Paul Young, University of Toronto)

Conclusions

- Remarkable and continuing computational and observational advances.
- Predictive models should build from empirical rules; rationalize and extend them.
- Advances will benefit all of rock mechanics.
- Waste isolation offers unprecedented opportunity to “know” the rock mass —Professor Müller’s prime concern.

Slides left out

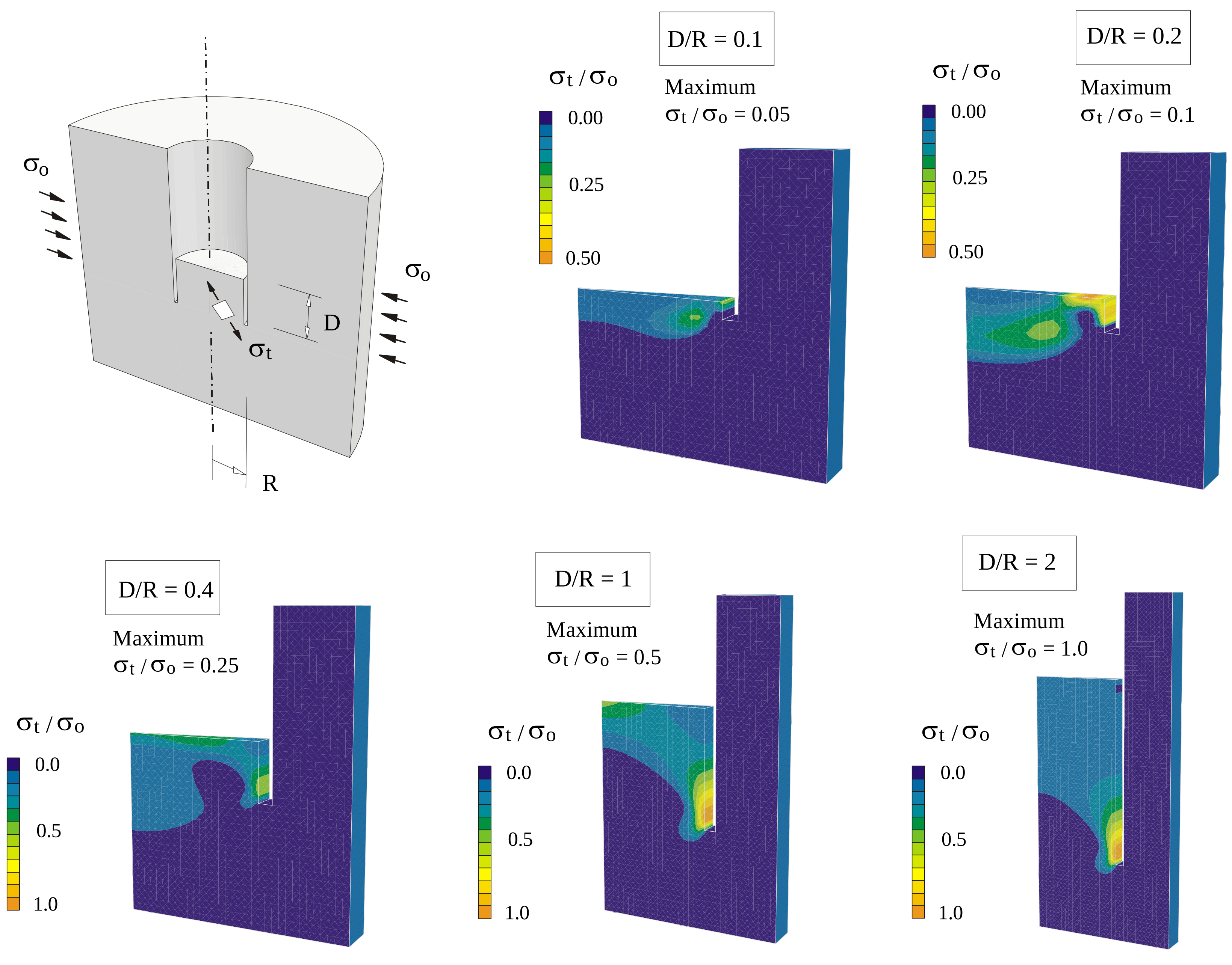

σ_o
σ_o
σ_t
D
R
D/R = 0.1
σ_t / σ_o
0.00
0.25
0.50
Maximum
σ_t / σ_o = 0.05
D/R = 0.2
σ_t / σ_o
0.00
0.25
0.50
Maximum
σ_t / σ_o = 0.1
D/R = 0.4
Maximum
σ_t / σ_o = 0.25
σ_t / σ_o
0.0
0.5
1.0
D/R = 1
Maximum
σ_t / σ_o = 0.5
σ_t / σ_o
0.0
0.5
1.0
D/R = 2
Maximum
σ_t / σ_o = 1.0
σ_t / σ_o
0.0
0.5
1.0